

CH4455 –Advanced Metal Chemistry: The Heavier Elements

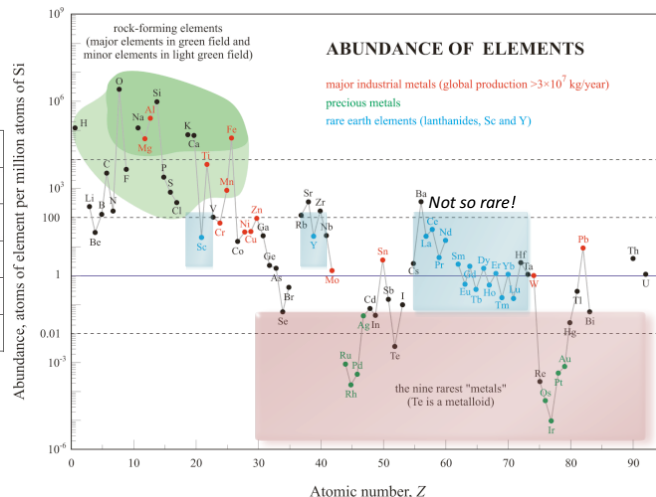
Distance Learning Material

Based on Advanced Metal Chemistry: The Heavier Elements in CH4514 in 2016-2017
Eli Zysman-Colman (ezc)

1. INTRODUCTION

The goal of this module is to understand concept and trends in the physical and photophysical properties of 4d, 5d and f-block elements. Introduction to concepts in photoredox catalysis and the use of metal complexes as drugs and diagnostic tools in medicine will also be covered.

1 H Hydrogen 1.008	2 He Helium 4.003											18 Ar Argon 39.948	19 K Potassium 39.098	20 Ca Calcium 40.078											36 Kr Krypton 83.801	37 Rb Rubidium 85.468	38 Sr Strontium 87.62											54 Xe Xenon 131.29	55 Cs Cesium 132.905	56 Ba Barium 137.327											86 Rn Radon 222	87 Fr Francium [223]	88 Ra Radium [226]
		D-BLOCK – TRANSITION METALS																																																			
		4d																																																			
		5d																																																			
		F-BLOCK – LANTHANOIDS																																																			
		F-BLOCK – ACTINOIDS																																																			



4f-elements are frequently referred to as rare-Earth elements. However, an evaluation of their relative abundance clearly makes this term a misnomer. In fact 5d elements are some of the most rare on Earth, with iridium being the most rare of the element with an atomic weight up to 94.

2. TRENDS ACROSS THE D-BLOCK

You have already seen several trends in physical properties across the d-block in CH2501 and CH3514. Here we will particularly concentrate on trends affecting the 4d and 5d elements. There are several global trends that can be discerned. For instance, with respect to the melting point (Mp), One can see that as the d-shell fills up to half filled, the Mp increases (exceptions Mn, Tc). This is because the strength of interatomic bonds is proportional to the number of half-filled d-orbitals. A more consistent trend in behaviour is observed for atomic (and ionic) radii. One can clearly observe that that the size of the neutral atoms decreases from left to right across the series, which is due to an increase in Z_{eff} with increasing atomic number. This trend is commonly known as the d-block (or scandide) contraction, which is a result of the poor shielding of the nuclear charge of d-electrons.

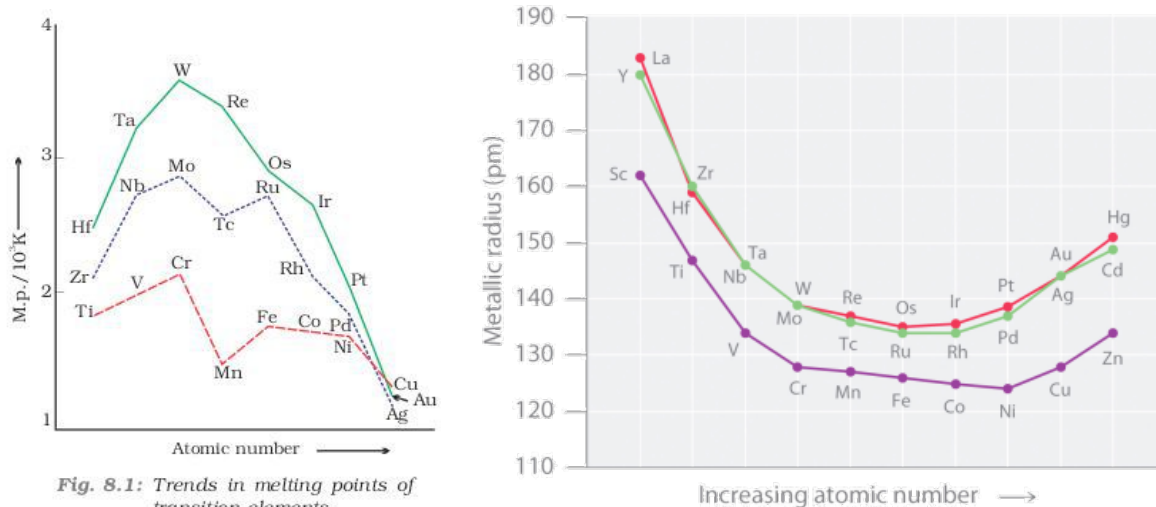


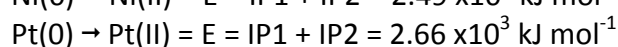
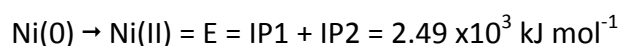
Fig. 8.1: Trends in melting points of transition elements

Further, one can also observe that the atomic radius increases going down the group from $3d < 4d < 5d$. However, this increase isn't linear. In fact the atomic radii of 4d and 5d elements is practically the same and both are larger across the group compared to 3d. This behaviour is the result of the lanthanoid contraction (see lanthanoid section for details). The same trends are also observed for ionic radii. The observed increase in atomic radii for d^8 , d^9 and d^{10} elements is due increased electron-electron repulsion.

Ionization potentials (IPs) measures the amount of energy required to remove an electron from an atom or ion. IPs therefore measure how strongly the atom or ion holds onto its electronics. IPs are proportional to $(Z_{\text{eff}})^2/n^2$ (where n is the principal quantum number). Generally, the first IP is smaller than the second, which is smaller than the third (and so on). As one removes electrons it takes more energy to remove the remaining electrons, which are themselves at lower energies as they are core electrons. The effect of increasing Z_{eff} across the period is partially mitigated by the increased shielding of the additional electrons. However, there are much smaller increases observed across the group, which is another manifestation of the lanthanoid contraction.

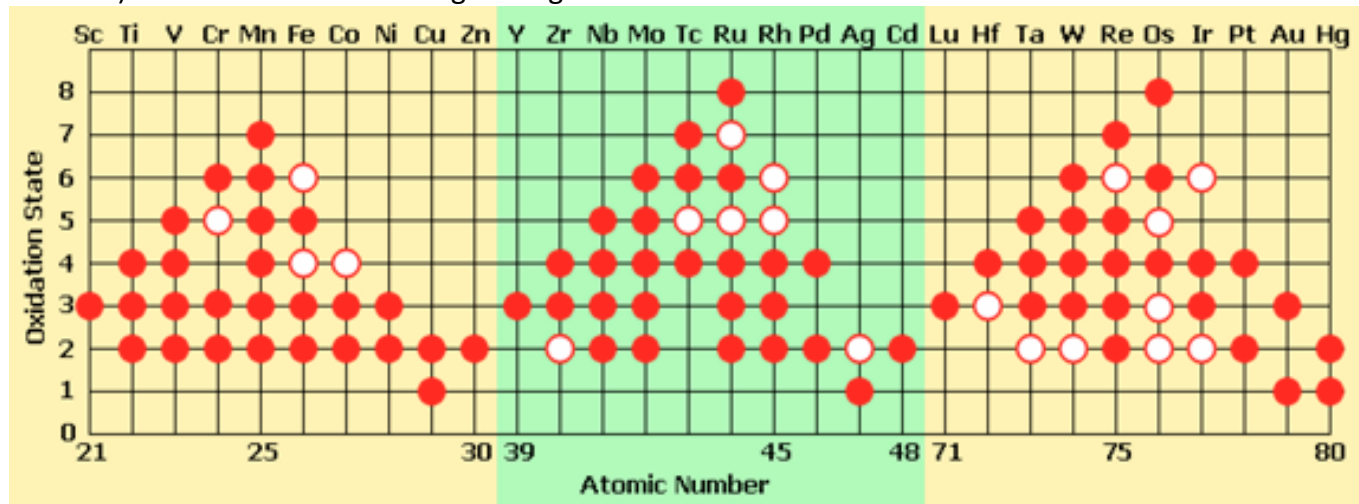
1											13	14	15	16	17	18		
1	H 1312.0																He 2372.3	
2	Li 520.2	Be 899.5											B 800.6	C 1086.5	N 1402.3	O 1313.9	F 1681.0	Ne 2080.7
3	Na 495.8	Mg 737.7	3	4	5	6	7	8	9	10	11	12	Al 577.5	Si 786.5	P 1011.8	S 999.6	Cl 1251.2	Ar 1520.6
4	K 418.8	Ca 589.8	Sc 633.1	Ti 658.8	V 650.9	Cr 652.9	Mn 717.3	Fe 762.5	Co 760.4	Ni 737.1	Cu 745.5	Zn 906.4	Ga 578.8	Ge 762.2	As 944.5	Se 941.0	Br 1139.9	Kr 1350.8
5	Rb 403.0	Sr 549.5	Y 599.9	Zr 640.1	Nb 652.1	Mo 684.3	Tc 702	Ru 710.2	Rh 719.7	Pd 804.4	Ag 731.0	Cd 867.8	In 558.3	Sn 708.6	Sb 830.6	Te 869.3	I 1008.4	Xe 1170.3
6	Cs 375.7	Ba 502.9	La 538.1	Hf 658.5	Ta 728.4	W 758.8	Re 755.8	Os 814.2	Ir 865.2	Pt 864.4	Au 890.1	Hg 1007.1	Tl 589.4	Pb 715.6	Bi 703.0	Po 812.1	At	Rn 1037.1
7	Fr 393.0	Ra 509.3	Ac 498.8	Rf 580	Db	Sg	Bh	Hs	Mt	Ds	Rg	Uub	Uut	Uuq	Uup			
			Lanthanides	Ce 534.4	Pr 528.1	Nd 533.1	Pm 538.6	Sm 544.5	Eu 547.1	Gd 593.4	Tb 565.8	Dy 573.0	Ho 581.0	Er 589.3	Tm 596.7	Yb 603.4	Lu 523.5	
			Actinides	Th 608.5	Pa 568	U 597.6	Np 604.5	Pu 581.4	Am 576.4	Cm 578.1	Bk 598.0	Cf 606.1	Es 619	Fm 627	Md 635	No 642	Lr 472.8	

With knowledge of IPs, it is possible to deduce which oxidation states are more thermodynamically stable. For instance $M(0) \rightarrow M(II) = E = IP1 + IP2$. The example below shows how this information is put into practice.

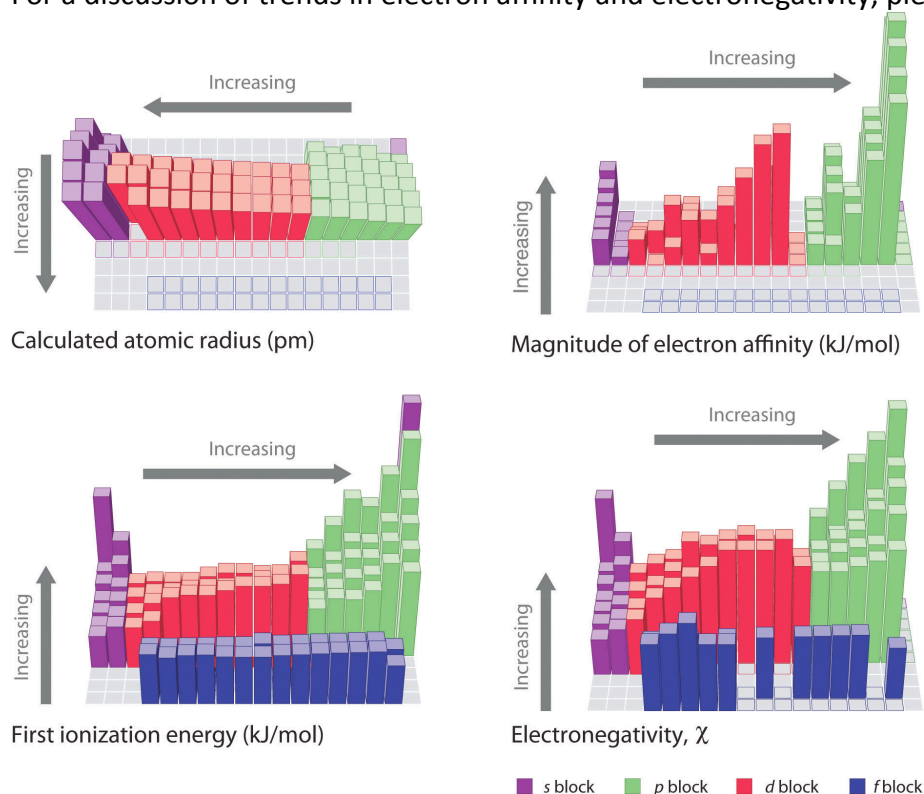


Therefore Ni(II) is more stable than Pt(II) as the amount of energy required to attain the +2 oxidation state is less for Ni than for Pt.

Elements with near half-filled d-shells can access many more oxidation states than those with either few or many d-electrons. Generally, lower oxidation state metals result in complexes with more covalent character to the M-L bond while this bond character becomes more ionic as the oxidation state of the metal increases. Higher oxidation states are more stable for heavier atoms. For instance, Mo^{VI} and W^{VI} are more stable than Cr^{VI} , with Cr^{VI} is the strongest oxidant of the three (i.e. it can most easily gain an electron). Ru and Os win for having the highest oxidation state at +8.



Globally, trends are as illustrated below. We have explored explicitly here trends in atomic radius and IP. For a discussion of trends in electron affinity and electronegativity, please refer to your notes in CH2501.



3. BASIC CONCEPTS IN LUMINESCENCE

The definition of luminescence is the emission of radiation followed by molecular excitation. There are many types of luminescence. These include:

- photoluminescence, where molecules are excited by photons of light;
- bioluminescence, which is luminescence that occurs in an organism;
- chemiluminescence, which is luminescence as a result of a chemical reaction (think luminol used to image blood stains in a crime scene);
- crystalloluminescence, which is luminescence that occurs during a crystallization event;
- mechanoluminescence, which is light emission as a result of mechanical work;
- electroluminescence, which is emission of light as a function of the application of an external bias (the basis for lighting devices such as OLEDs);
- cathodoluminescence, which is emission of light from matter when irradiated with electrons;
- radioluminescence, which is alpha, beta and gamma radiation causing luminescence;
- thermoluminescence, which is luminescence that results when the material is heated; and
- sonoluminescence, which is light emission that results from excitation by sound waves.

Photoluminescence (PL) in particular involves radiative decay (i.e. emission of light) from a molecule in its excited state (M^*) after it has been excited through the absorption of energy – $M^* \rightarrow M$.

3.1 Quick Review on Selection Rules for Electronic Transitions

- **Spin selection rule**
The electromagnetic field of the incident radiation cannot change the relative orientation of the spins of the electrons in a compound. This rule relaxes in the presence of spin-orbit coupling.
 $\Delta S = 0$; **spin-allowed**
 $\Delta S \neq 0$; **spin-forbidden**
- **Laporte (angular momentum) selection rule**
In a centrosymmetric molecule or ion, the only allowed transitions are those accompanied by a change in parity. In other words, transitions between g and u terms are permitted.
s-s, p-p, d-d, f-f, $\Delta l = 0$; **Laporte-forbidden**
s-p, p-d, d-f, $\Delta l = 1$; **Laporte-allowed**

3.2 Orbitals vs. States

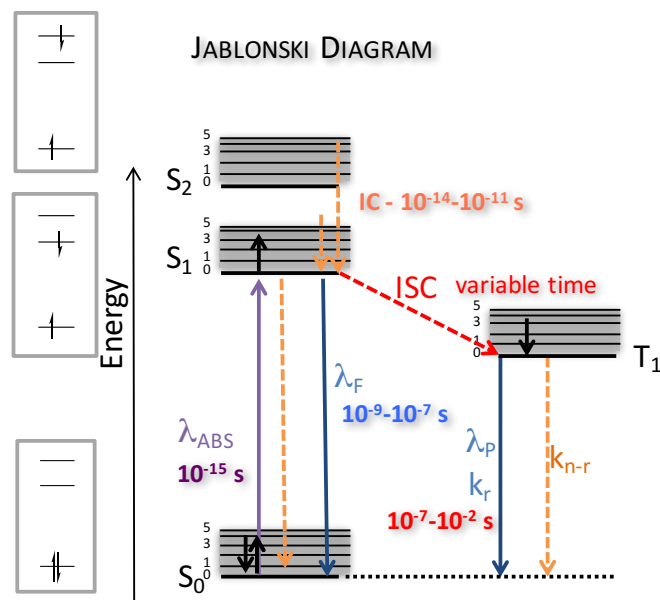
Orbitals describe the location and energy of individual electrons. Electronic transitions involve the excitation from one orbital to another orbital that is at higher energy compared to the first. States describe the total energy and overall electronic configuration of the whole molecule. The lowest energy configuration is called the **ground state** (S_0) and has singlet multiplicity. All other configurations are called **excited states** (S_n or T_n , where $n > 0$); S stands for singlet and T stands for triplet. A molecule in a Singlet state has $\Delta S = 0$ (i.e. all electrons have paired spins) while a molecule in a Triplet state has $\Delta S = 1$.

3.3 Absorption

There are three types of absorption to consider: rotational, vibrational and electronic. Electronic absorption involves exciting an electron from an occupied orbital to an unoccupied (or partially occupied) orbital. The excited states are treated in the "localized MO approximation": the transition is considered to involve two predominant orbitals, the electron being promoted from MO_1 to MO_2 , ignoring more or less the other orbitals. The absorption bands observed in an absorption spectrum correspond to the electronic transitions.

Recall that absorption, A , is related to Transmittance, T . The absorption is proportional to the molar absorptivity, ϵ , the concentration, c and the path length, l , by which the light passes through the sample. This relationship is known as the **Beer-Lambert Law** and is given by: $T = I / I_0$; $A = -\log T = \epsilon cl$

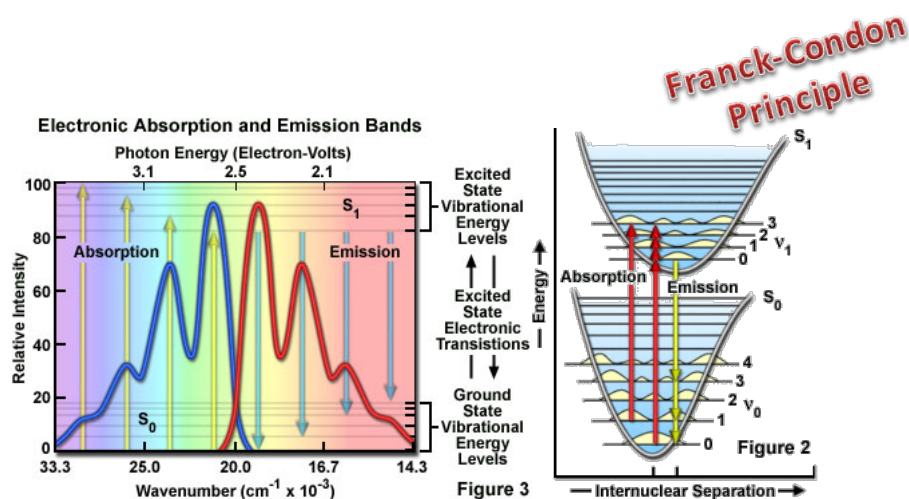
3.3 Jablonski Diagram



S_2 states.

The photophysical processes that occur during absorption and emission of light are normally represented in a Jablonski diagram (above). The diagram is named after Alexander Jablonski, widely regarded as the father of fluorescence spectroscopy. The singlet ground state (S_0) and first (S_1) and second (S_2) singlet excited states are shown as is the first triplet (T_1) excited state. At each of these electronic energy levels, the molecule can exist in a number of vibrational energy levels (denoted by 0, 1, 2 ...). Also denoted to the left of the Jablonski diagram are the molecular orbitals most likely involved in the population of the valence electrons in the S_1 and

Transitions between states are shown as vertical lines to illustrate the essential instantaneous nature of the light absorption. In fact light absorption occurs in about 10^{-15} s, a time too short to permit nuclear movement. This concept is known as the **Franck-Condon principle**. Depending on the energy of the light absorbed, the electron can be excited to $S_1, S_2 \dots S_n$ electronic excited states and can, within each of those states, access different vibrational levels. Several processes can now occur, but with very few exceptions, electronic (and vibrational) relaxation to the lowest vibrational level of the S_1 state rapidly occurs via a process known as **internal conversion (IC)**. IC normally occurs in 10^{-14} to 10^{-11} s. This non-radiative decay mode is denoted by dashed lines in the Jablonski diagram. From the S_1 state, molecules can then emit light *via fluorescence*, returning to the ground state (S_0) but likely at an excited vibrational state at that level. Fluorescence normally occurs on the nanosecond timescale. A consequence of fluorescence occurring to higher vibrational ground states is that the fluorescence spectrum is typically the **mirror image** of the absorption spectrum of the $S_0 \rightarrow S_1$ transition (see below). This similarity occurs as electronic excitation does not perturb nuclear geometry. This is a further manifestation of the Franck-Condon principle. From this description, one can observe that there will be the same fluorescence energy regardless of the excitation energy used. This near universal property is known as **Kasha's Rule**. The energy difference between lowest energy absorption band and the highest energy emission band is known as the **Stokes Shift**. Stokes shifts for fluorescent molecules are generally much smaller than those for phosphorescent molecules. This is because the triplet state is always lower in energy than the singlet state. Though the reasoning is complex, one way to rationalize this observation is to invoke Hund's rule. In the singlet state, the two electrons are paired, which raises the energy of the state compared to the triplet state.



Another option aside from fluorescence once the molecule is in the S_1 state is for the molecule to undergo a spin conversion to the triplet state (T_1) in a process known as **intersystem crossing** (ISC). Emission from the triplet state is termed **phosphorescence**. As phosphorescence is formally from a spin-forbidden state ($\Delta S \neq 0$), the time that it takes is generally much longer and ranges from 10^{-7} to 10^{-2} s. Molecules containing heavy atoms such as d-block metals are frequently phosphorescent. This is due to their relatively large spin-orbit coupling (SOC) constants, which facilitate ISC.

Apart from these decay modes, Förster, Dexter or radiative energy transfer to other molecules are possible as is electron transfer in lieu of radiation. The excited state can also non-radiatively relax back down to the ground state (k_{nr}). The efficiency of the emission, denoted by the photoluminescence quantum yield (Φ_{PL}) is the ratio of the radiative decay modes (i.e. fluorescence and phosphorescence) to all these other decay modes. It should be noted that emission is red-shifted (*bathochromic*) relative to the absorption and absorption is likewise blue-shifted (*hypsochromic*) relative to the emission.

3.4 Important types of electronic transitions

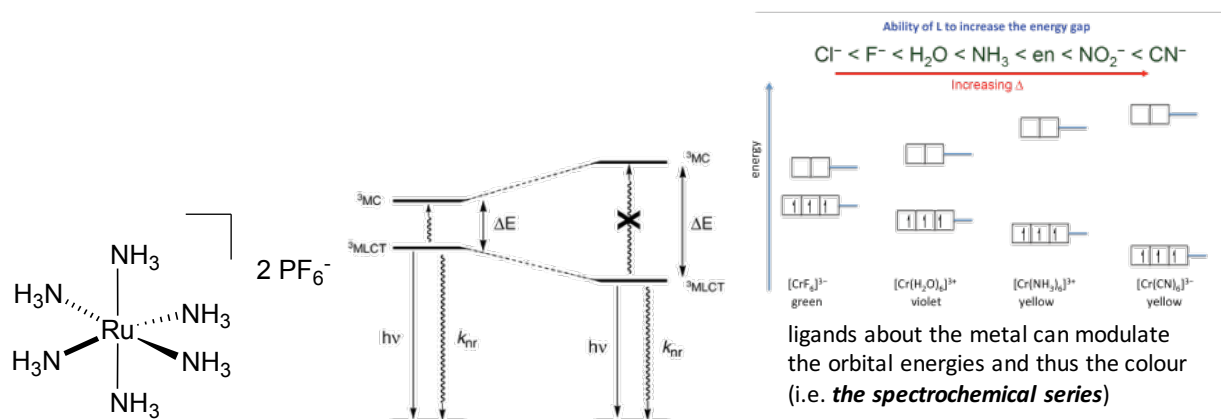
In an organometallic complex there are different classes of electronic transitions (be it *via* absorption or emission). The most common of these are listed below but this is not an exhaustive list:

- metal-centered (MC), where an electron transitions from one metal orbital to another (i.e. $d \rightarrow d$)
- ligand-centered (LC), where an electron transitions from one ligand-based orbital to another without large redistribution in the electron density (i.e. $\pi \rightarrow \pi^*$)
- metal-to-ligand charge transfer (MLCT), where an electron transitions from a metal orbital to a ligand-based antibonding orbital (i.e. $d \rightarrow \pi^*$)
- ligand-to-metal charge transfer (LMCT), where an electron transitions from an occupied ligand-based orbital to an unoccupied metal orbital (i.e. $\pi \rightarrow d$)

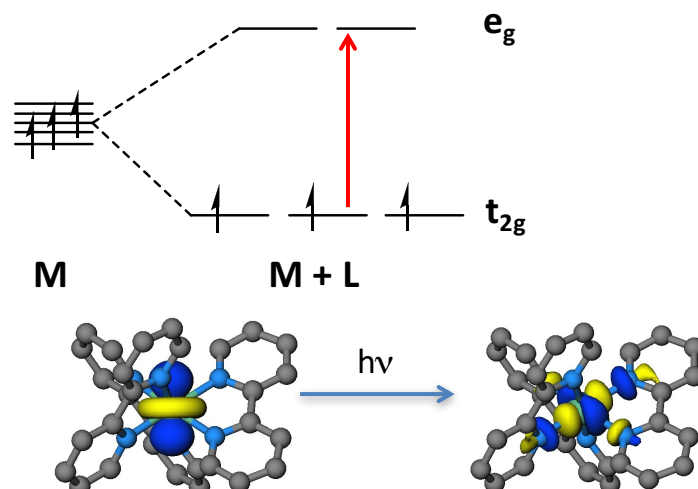
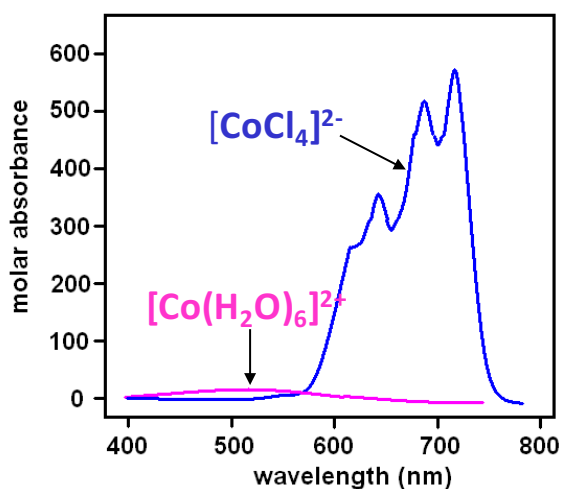
3.4.1 Metal-centered (MC) transitions

These sorts of transitions are frequently observed for 3d-metal complexes, where the energy difference between metal-based orbitals (Δ) is not large. This energy difference can however be modulated by the ligand field around the metal, frequently passing through all the colours of the visible spectrum, which is known as the **spectrochemical series**. Practically speaking, the degree to which ligands can tune the

energy difference of the d-orbitals is a function of their σ -donating, π -donation and π -accepting properties.



Frequently, the lowest energy transition will involve d→d excited states, which are typically non-emissive due to significant perturbations in the bonding geometry around the metal center upon reorganization of the metal d electrons. Such complexes are typically very poorly absorptive (Laporte forbidden transitions) and are non-emissive. MC transitions become more intense and are broadened by the effects of molecular vibrations, which distort the crystal field and makes these transitions more allowed (see below).



An example of such a complex is $[\text{Ru}(\text{NH}_3)_6]^{2+}$. Importantly, MC states can still be accessed even if they are not the lowest energy transitions. This is because at room temperature, there may be enough thermal energy to populate a higher lying MC state and from there to non-radiatively decay back to the ground state.

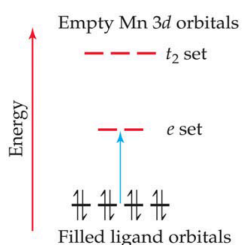
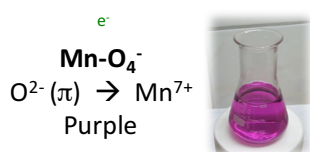
These states are dissociative, because an antibonding orbital is populated by the electronic transition. Two classical examples:

- $\text{Ti}(\text{H}_2\text{O})_6^{3+}$: the electronic configuration of Ti(III) is d^1 . This implies that, to generate the excited state, the electron be taken from a t_{2g} -orbital so as to populate an e_g^* level, which is strongly antibonding.

- $\text{Rh}(\text{NH}_3)_6^{3+}$: the electronic configuration of Rh(III) is d^6 . To generate the excited state, the electron has also to be taken from a t_{2g} -orbital to populate an e_g^* level, which is strongly antibonding).

If $\text{Rh}(\text{NH}_3)_6^{3+}$ were excited in water for instance then $[\text{Rh}(\text{NH}_3)_6^{3+}]^*$ (the * refers to an excited species) is rapidly aquated. The complex itself is actually thermally very stable. The excited state is 10^{14} times more reactive than the ground state! MC states are not adapted to photosynthesis and photoredox reactions in general. On the other hand, if we want to exchange ligands under the action of light, they could be particularly useful (i.e. light-driven machines and motors)

3.4.2 Ligand-to-metal charge transfer (LMCT) transitions

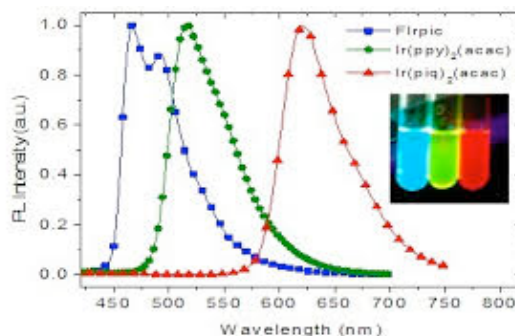
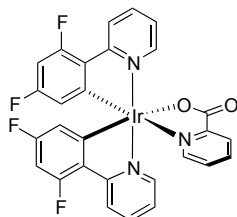
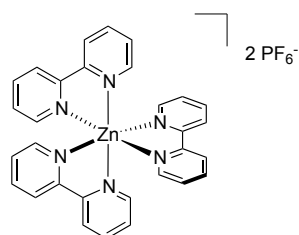


Complexes with LMCT transitions exhibit very intense absorption bands ($\epsilon > 1000 \text{ L}^{-1} \text{ cm}^{-1}$). As there is the movement of an electron from a ligand to the metal, there is a large transition dipole moment. LMCT bands are typically broad and unstructured. LMCT transitions are very solvatochromic. Typically, though these complexes are brightly coloured they are typically non-emissive. Complexes that possess metals in high oxidation states and/or very electron rich ligands are prone to show LMCT transitions. Examples include: $[\text{Co}^{\text{III}}(\text{NH}_3)_5\text{Br}]^{2+}$, $[\text{Ir}^{\text{IV}}\text{Cl}_6]^{2-}$, $[\text{MnO}_4]^-$ (see left).



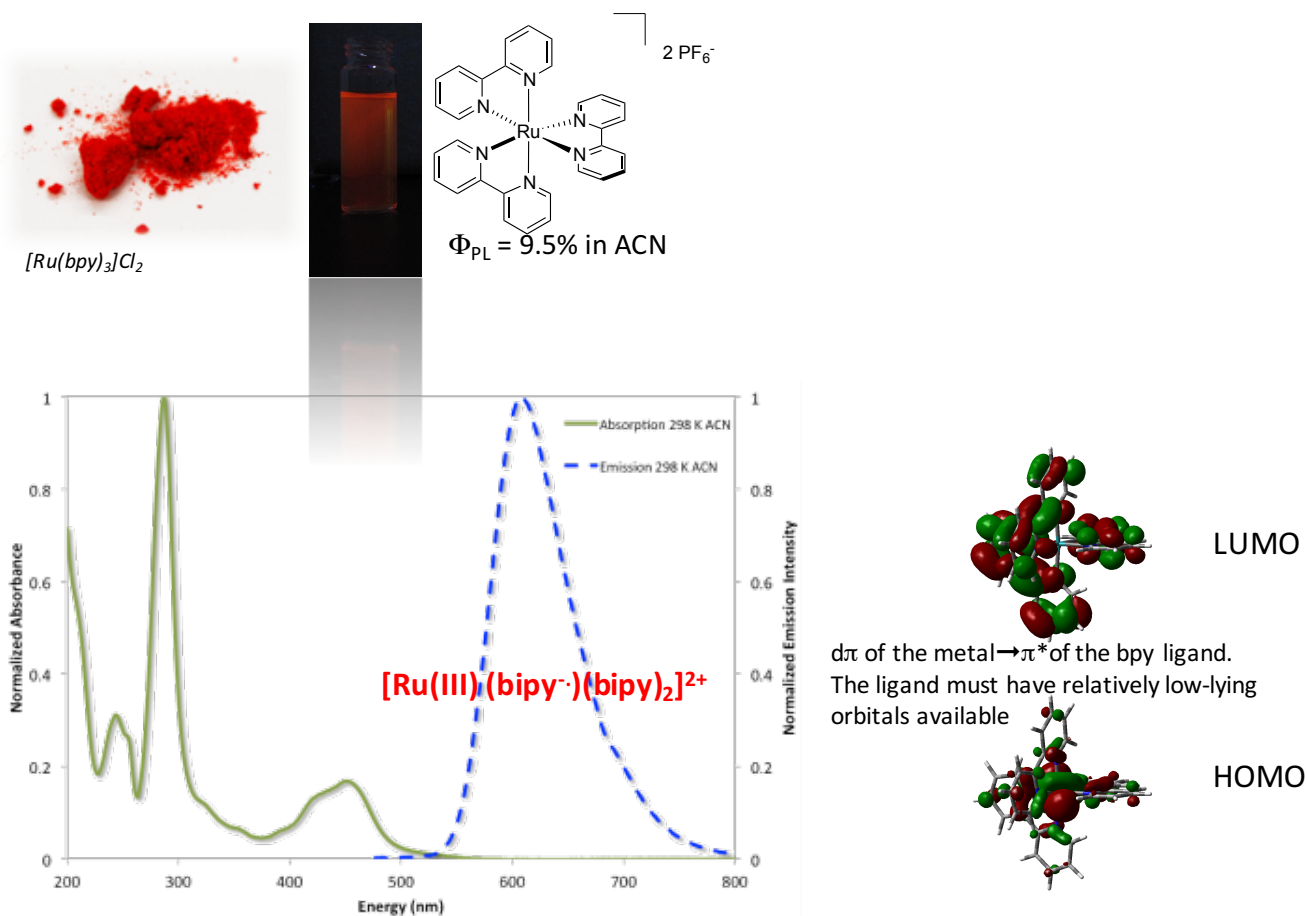
3.4.3 Ligand-centered (LC) transitions

Complexes with LC transitions typically show very intense absorption bands ($\epsilon > 10,000 \text{ L}^{-1} \text{ cm}^{-1}$). Emission can likewise be very intense. Both the absorption and emission spectra show fine structure, which is the result of observed emission (or absorption) from the same electronic transition but from multiple vibrational levels. Examples of complexes exhibiting LC transitions include: $[\text{Zn}(\text{bpy})_3]^{2+}$ and $[\text{Ir}(\text{dFppy})_2\text{pic}]$, the latter commonly known as Irpic (shown below). Notice in the emission spectra on the right how Irpic shows two distinct bands while the other two complexes show unstructured emission. This is the common signature for LC emission.



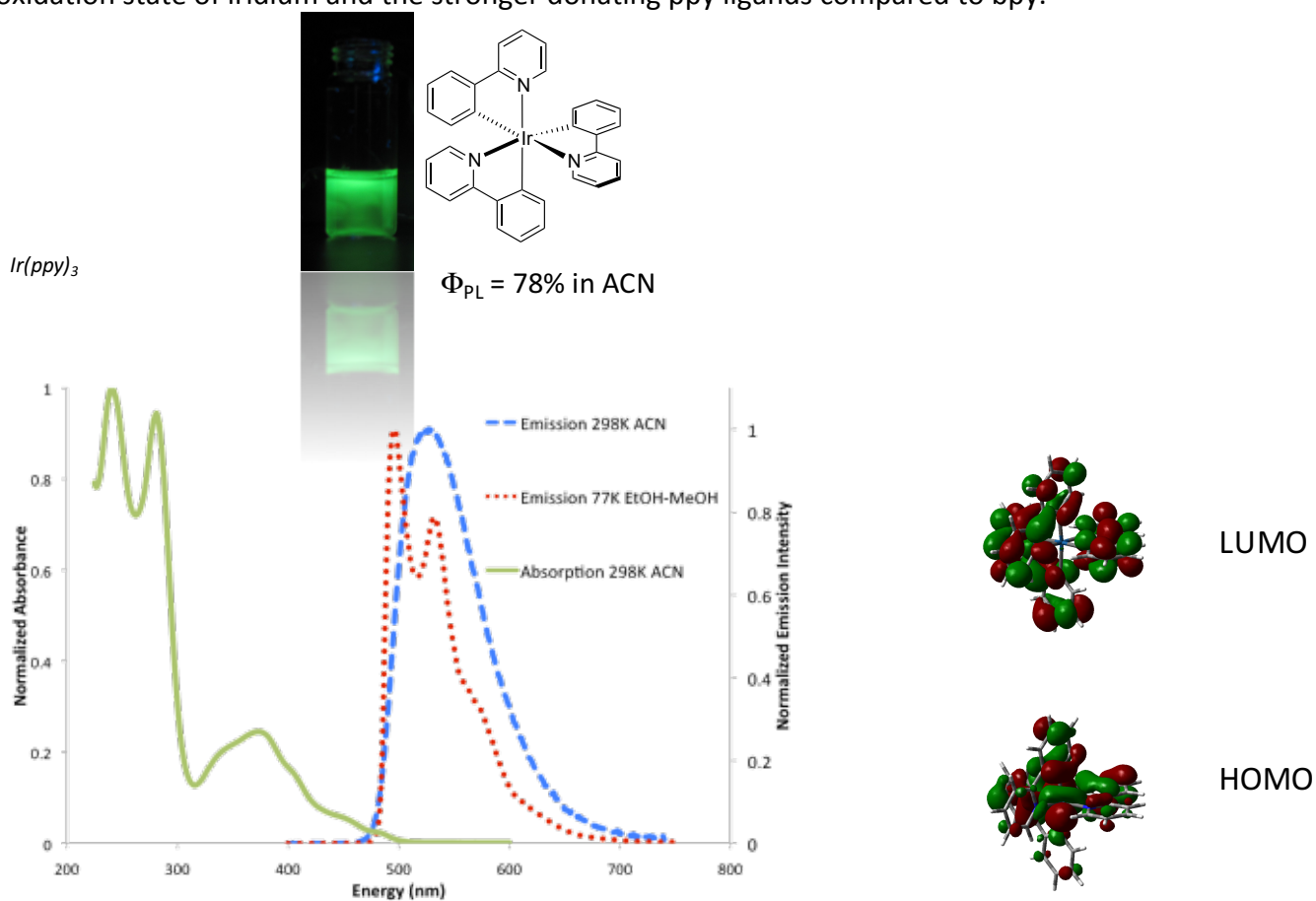
3.4.4 Metal-to-ligand charge transfer (MLCT) transitions

Similar to LMCT transitions, MLCT absorption transitions possess large molar absorptivities ($\epsilon > 1000 \text{ L}^{-1} \text{ cm}^{-1}$) as a consequence of the fact that the complexes possess large transition dipole moments. Emission intensity can also be very intense. Both absorption and emission are solvatochromic and their profiles are typically broad and unstructured. MLCT transitions tend to occur with electron-poor ligands and relatively low oxidation state for the metal (e.g., $\text{Re}(\text{bpy})(\text{CO})_3\text{Cl}$, $\text{Mo}(\text{bpy})(\text{CO})_4$). The archetypal example of a complex showing MLCT behaviour is $[\text{Ru}(\text{bpy})_3]^{2+}$. The MLCT absorption band can be found at 450 nm while the emission occurs at around 610 nm in MeCN. During excitation, an electron from a metal-based orbital (d_{z^2} in this case) moves to one of the three bpy ligands, thus generating an oxidized Ru center and a one-electron reduced bpy ligand (essentially a radical anion).

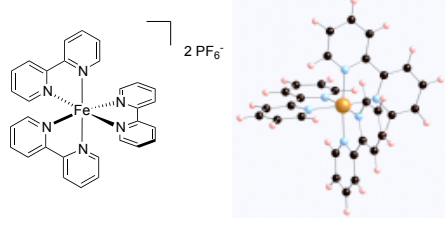


Another famous example of a complex that show MLCT behaviour is *fac*- $\text{Ir}(\text{ppy})_3$. Here too upon excitation the electron moves from an iridium-based metal orbital to one the pyridine rings of one of

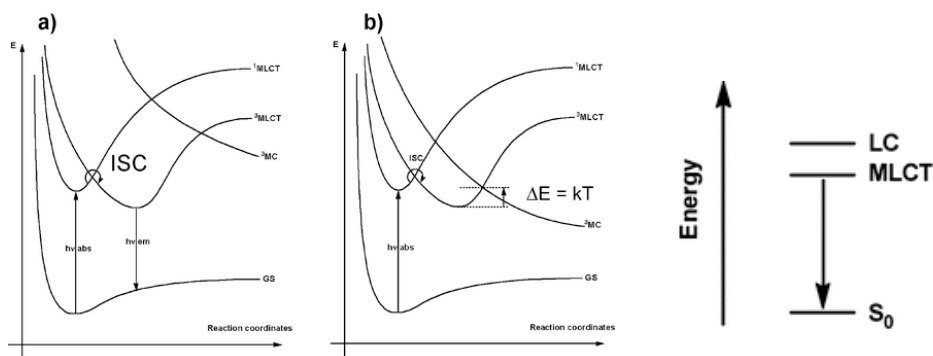
the 2-phenylpyridine ligands. $\text{Ir}(\text{ppy})_3$ is juxtaposed to $[\text{Ru}(\text{bpy})_3]^{2+}$ in that it is significantly brighter and blueshifted in its emission (and absorption). This is partially a result of the fact that iridium is 5d compared to ruthenium, which is 4d (greater splitting of metal-based orbitals), as well as the 3+ oxidation state of iridium and the stronger donating ppy ligands compared to bpy.



Contrast the enhanced emission observed here to $[\text{Fe}(\text{bpy})_3]^{2+}$, which is very poorly emissive. Though the complex is strongly absorptive, the presence of thermally accessible MC states (due to poorer splitting of the d-orbitals as it is a 3d metal) provides a non-radiative quenching route for the emission.

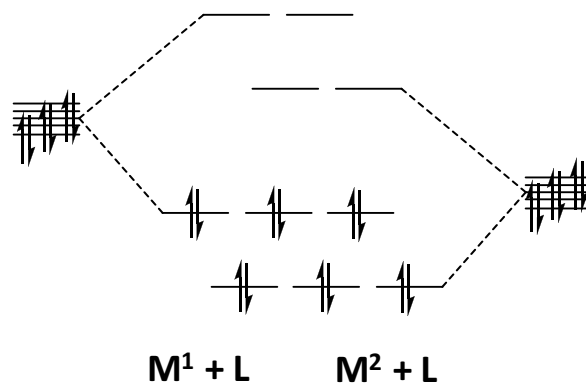
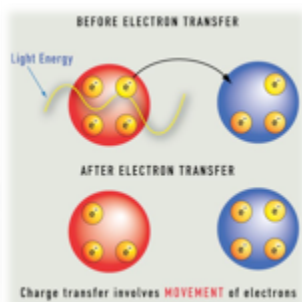


strongly purple solution but non-emissive

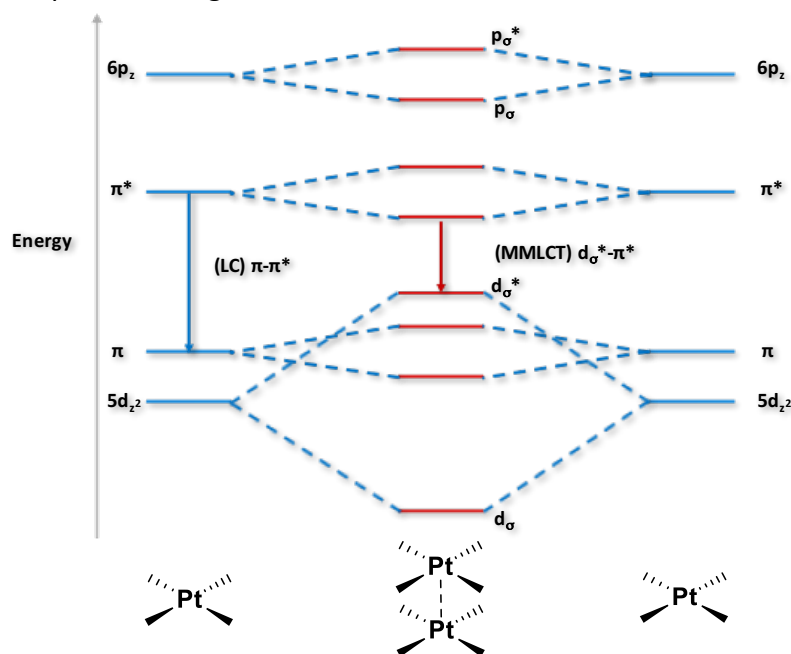


3.4.5 Metal-to-metal charge transfer (MMCT) transitions

MMCT transitions, also known as intervalence charge transfer occurs in complexes with two or more metal centers. Upon excitation, an electron moves from the occupied d-orbitals of one metal to the unoccupied d-orbitals of another (below, right). Indeed the blue colour of sapphires is due to an MMCT transition between between Fe^{2+} and Ti^{4+} metal ions in the gem.

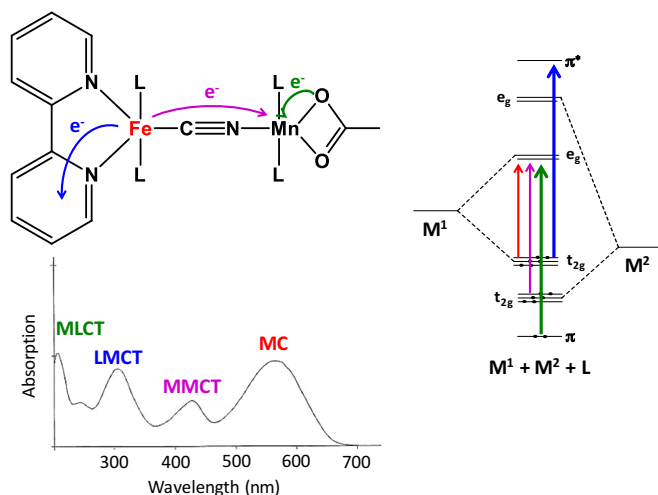


Platinum(II) complexes frequently show MMCT transitions at elevated concentrations. This is due to the d_{z^2} orbitals of adjacent square planar complexes interacting with each other in a σ -bonding fashion, resulting in the formation of a new bond. MMCT transitions can now occur between the two platinum centers. Notice in the MO diagram that the new MMCT transition is much lower in energy than any available transition on the isolated Pt complexes. Thus, significantly red-shifted emission in these complexes is diagnostic of MMCT transitions.



3.4.6 Complexes with multiple transitions

Frequently, the nature of the photophysics of a particular complex is complex. There can be multiple different absorption transitions, all of which are a consequence of the structure of the complex. The example below illustrates this point where MLCT, LMCT, MMCT and MC transitions can all be observed in the absorption spectrum.



4 Photoredox catalysis

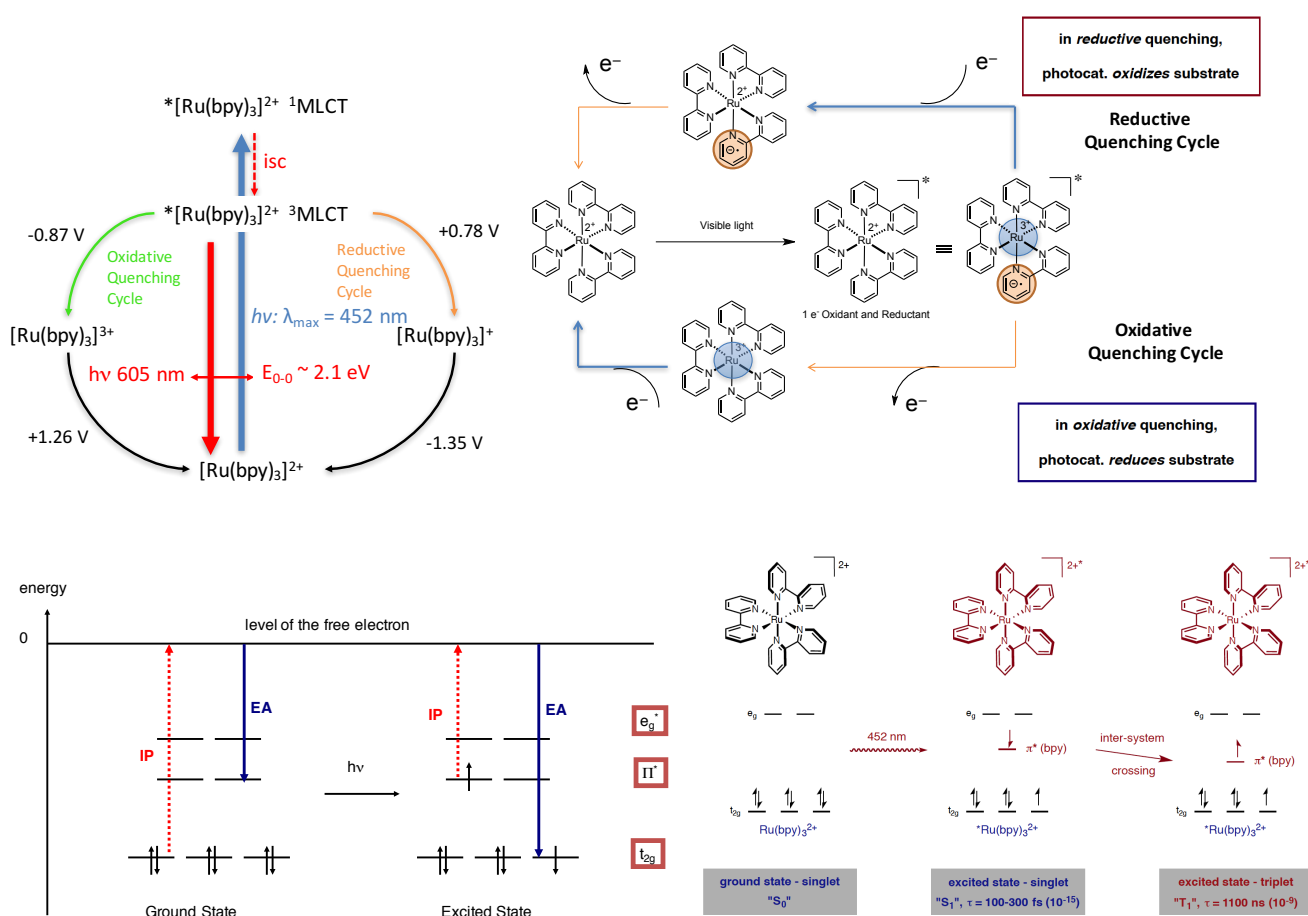
Photochemistry has been around for over 100 years, by which it is meant that light can be used as a reactant to generate molecular reactive species. Examples of photochemical reactions include the Paterno-Büchi reaction of dimerization of acetone and [2+2] cycloaddition reactions mediated by light. In these types of reactions, high-energy ultra-violet light and special quartz glassware are required. Photoredox catalysis globally refers to the use of a photosensitizer material added in order to initiate these photochemical reactions but at much lower excitation energy. The use of photophysically-active complexes as photoredox catalysts (**PRC**) has become very popular of late. This is due to the fact that upon photoexcitation, the excited state of the complex is generally a better oxidant and a better reductant than the ground state, which sounds like a paradoxical statement but in fact isn't. There are many advantages to using PRCs: often they provide unique reactivity, afford mild single electron chemistry, are considered "green" and use of visible light without the need for special glassware, permit mild reaction conditions, and allow for tunable electronic properties of the photocatalysts as a function of the nature of the metal and ligands.

4.1 [Ru(bpy)₃]²⁺: the archetypal PRC

[Ru(bpy)₃]²⁺ is one of the most popular PRCs. It will be used to illustrate a photoredox catalytic cycle below. Upon photoexcitation at 452 nm, [Ru(bpy)₃]²⁺ gets excited into its singlet ¹MLCT state. Through rapid ISC, the excited triplet ³MLCT state is populated. We have already seen that if nothing else is present, the complex will radiative relax and emit light at around 605 nm. However, in the presence of a secondary reactant (which in photoredox catalysis is an organic molecule) *[Ru(bpy)₃]²⁺ can either donate (**oxidative quenching cycle**) or receive (**reductive quenching cycle**) an electron. Through the oxidative quenching cycle, the electron from the radical anion on one of the bpy ligands is transferred to the organic substrate, thereby generating a formally [Ru(bpy)₃]³⁺ oxidized PRC and a reduced substrate. In the presence of a sacrificial reductant (frequently a secondary reactant), [Ru(bpy)₃]³⁺ can be reduced back to [Ru(bpy)₃]²⁺ thus completing the catalytic cycle. Through the reductive quenching cycle an electron is transferred from the organic reactant to the metal of the complex, thereby reducing the complex formally to [Ru(bpy)₃]⁺ (in actuality Ru is in the 2+ oxidation state and there is still the radical anion on one of the bpy ligands) and oxidizing the substrate. [Ru(bpy)₃]⁺ can be reoxidized to

$\text{Ru}(\text{bpy})_3^{2+}$ in the presence of a sacrificial oxidant (frequently a secondary reactant) to complete the catalytic cycle.

Thermodynamically speaking, the energy required to remove (oxidize) or add (reduce) the complex in solution may be measured by cyclic voltammetry experiments. For $\text{Ru}(\text{bpy})_3^{2+}$ it takes 1.26 V to oxidize the complex and -1.35 V to reduce the complex. The excited state oxidative (and reductive) energy is the difference between the triplet state energy (which is 2.1 eV for $\text{Ru}(\text{bpy})_3^{2+}$) and the ground state redox chemistry. Thus, for the oxidative quenching cycle it is -0.87 V while for the reductive quenching cycle it is 0.78 V. This is the embedded energy available to either reduce or oxidize the organic reactant, respectively. EA, the electronic affinity, is directly related to the oxidizing character of the complex, whereas the ionisation potential, IP, is roughly inversely proportional to its reducing power and, simplistically, is schematically outlined below.

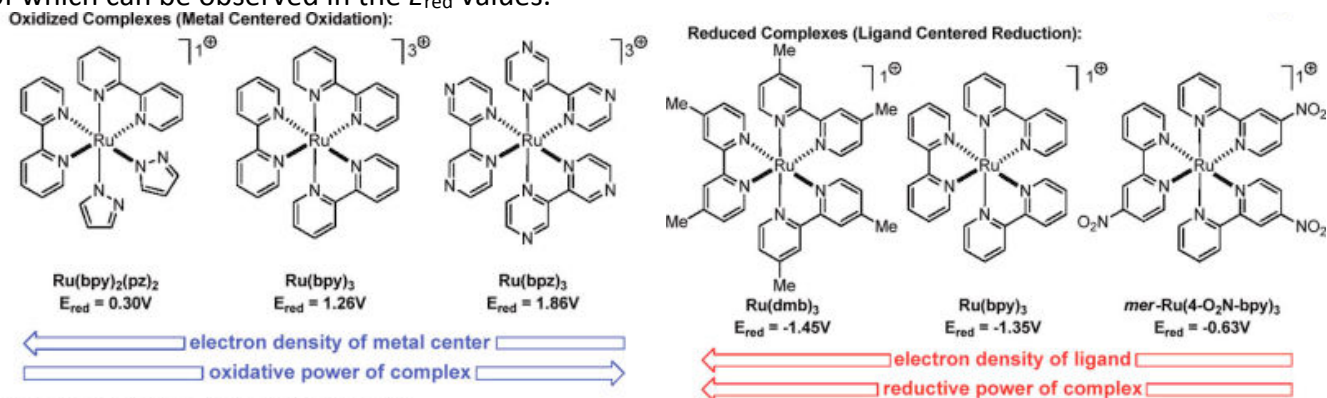


4.1.1 Tuning the electronics of the PRC

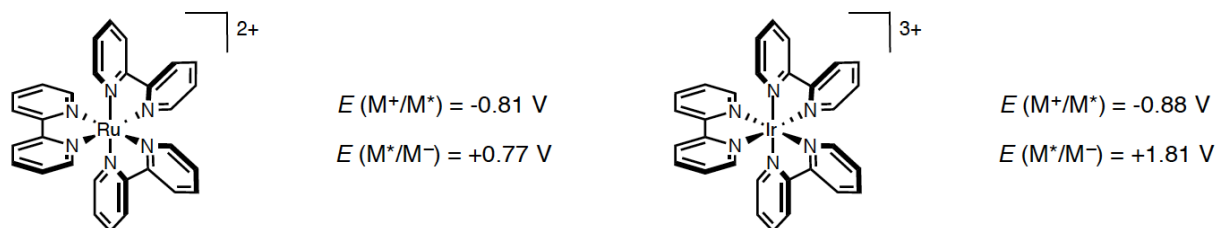
Recall that the HOMO for $\text{Ru}(\text{bpy})_3^{2+}$ is located on the Ru center while the LUMO is located on the bpy ligands. Thus, if we modulate the electronics of the ligand, we will be able to tune these orbitals. Importantly, the HOMO energy can be modulated as by tuning the electronics of the ligands, we are tuning their σ -donating character, which will impact the energy of the metal d-orbitals. The examples below illustrate how both HOMO and LUMO energies can be modulated (the tuning of HOMO and LUMO energies is frequently coupled, meaning that though for illustration purposes we will see how to

tune one or the other of these orbitals, it does not mean that the other is not also being tuned at the same time).

Replacement of bpy for bipyrazine, which is a more electron poor ligand, stabilizes the HOMO while the use of electron-rich pyrazolate ligands raises the HOMO. This can be observed in the E_{ox} values (image is incorrect the values are E_{ox}). Analogously, placing inductively electron-donating methyl groups destabilizes the LUMO while placing electron-withdrawing nitro groups stabilizes the LUMO, the effects of which can be observed in the E_{red} values.



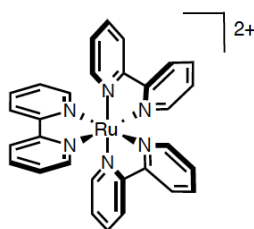
Increasing the charge and electronegativity of the metal affects the redox potentials.



$Ru(bpy)_3^{2+}$ – weaker oxidant, stronger reductant

$Ir(bpy)_3^{3+}$ – similar reductant, much stronger oxidant

Below is a summary of the relevant optoelectronic properties of some of the most widely used photoredox catalysts. Note how as the cyclometalating ligand becomes more electron poor, the HOMO is stabilized in the Ir complexes and the PRC becomes more oxidizing.

 $Ru(bpy)_3^{2+}$

$E(M^+/M^*) = -0.81 \text{ V}$

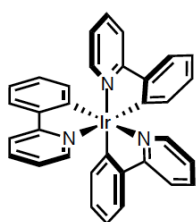
$E(M^*/M^-) = +0.77 \text{ V}$

$\tau = 1.1 \mu\text{s}$

$\lambda_{abs} = 452 \text{ nm}$

$\lambda_{em} = 652 \text{ nm}$

$\Phi_{em} = 0.095$

 $Ir(ppy)_3$

$E(M^+/M^*) = -1.73 \text{ V}$

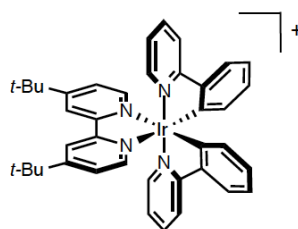
$E(M^*/M^-) = +0.31 \text{ V}$

$\tau = 1.9 \mu\text{s}$

$\lambda_{abs} = 375 \text{ nm}$

$\lambda_{em} = 518 \text{ nm}$

$\Phi_{em} = 0.38$

 $Ir(ppy)_2(dtbbpy)^{2+}$

$E(M^+/M^*) = -0.96 \text{ V}$

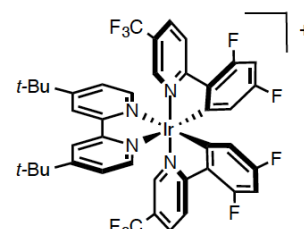
$E(M^*/M^-) = +0.66 \text{ V}$

$\tau = 0.56 \mu\text{s}$

$\lambda_{abs} = 410 \text{ nm}$

$\lambda_{em} = 581 \text{ nm}$

$\Phi_{em} = 0.094$

 $Ir[dF(CF_3)ppy]_2(dtbbpy)^+$

$E(M^+/M^*) = -0.89 \text{ V}$

$E(M^*/M^-) = +1.21 \text{ V}$

$\tau = 2.3 \mu\text{s}$

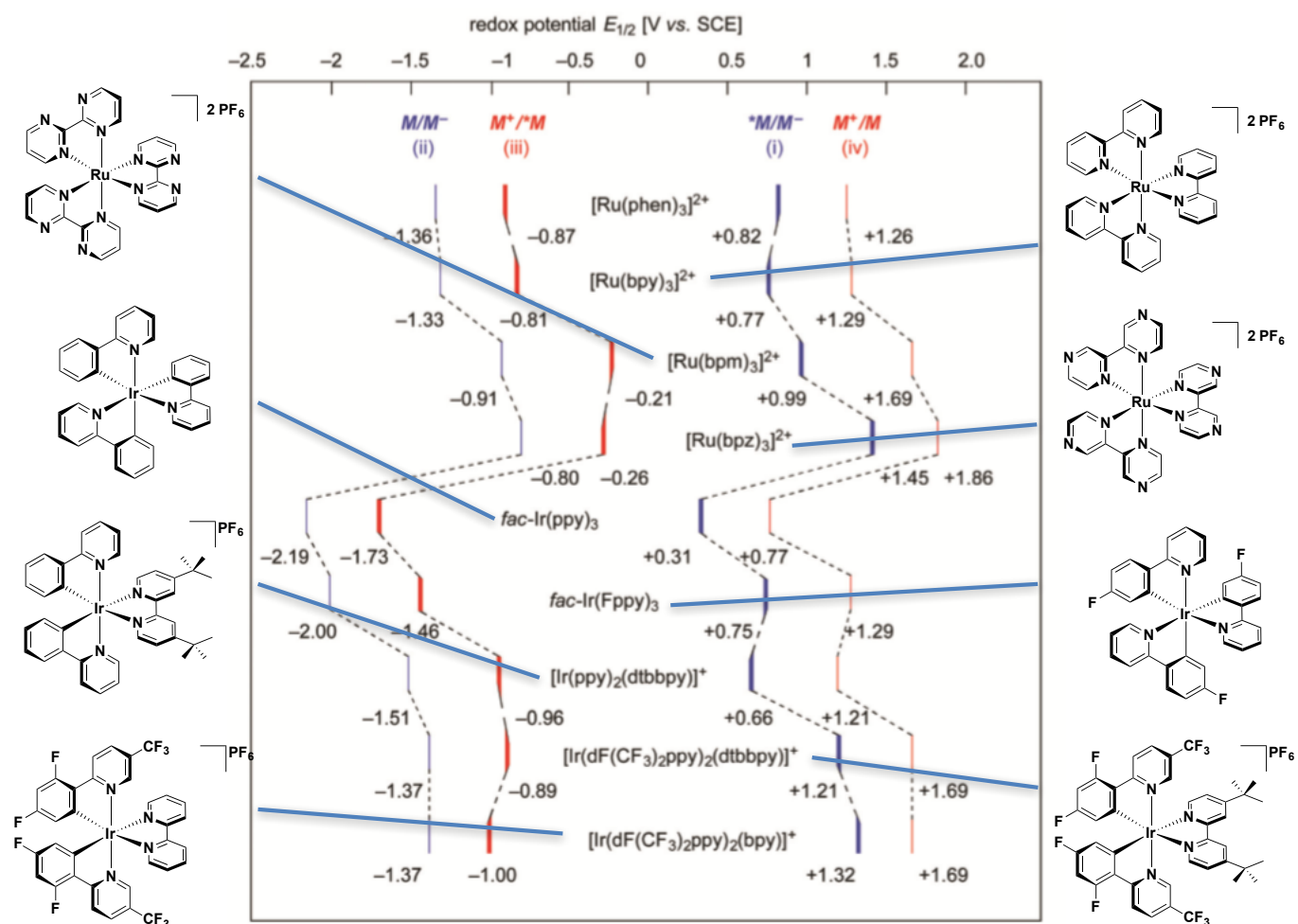
$\lambda_{abs} = 380 \text{ nm}$

$\lambda_{em} = 470 \text{ nm}$

$\Phi_{em} = 0.68$

strong reductants have $E_{1/2}(M^+/M^*) < -1.5$, strong oxidants have $E_{1/2}(M^*/M^-) > +1.2$

For $Ir(ppy)_3$ and the heteroleptic iridium complexes the HOMO is located on the Ir and the phenyl ring of the cyclometalating ligands. The LUMO in $Ir(ppy)_3$ is located on the pyridine ring while the LUMO of the cationic iridium complexes is located on the bipyridine ancillary ligand. See below for further examples of how the ground and excited state redox potentials are influenced by the structure of the PRC.



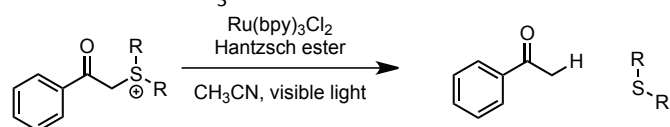
4.2 Brief history of photoredox catalysis

1936: Burstall

First report of $[Ru(bpy)_3]^{2+}$ and resolution of its enantiomers

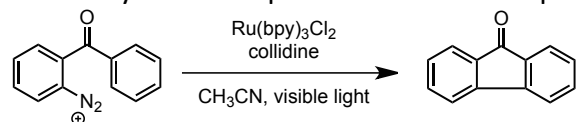
1978: Kellogg

$[Ru(bpy)_3]^{2+}$ is used as a catalyst. Reaction is induced by visible light!



1984: Deronzier

Synthesis of phenanthrenes via a photocatalytic Pschorr reaction



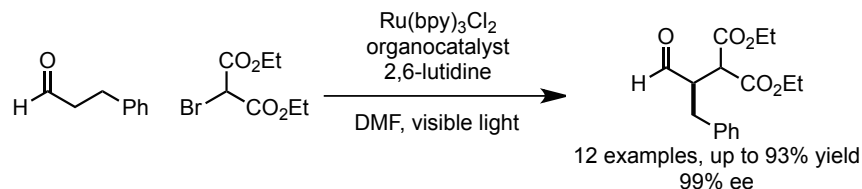
1999: Kodadek

Photo-triggered oxidative protein cross-linking of tyrosine residues
Other contributions from Fukuzuni, Okada and Barton

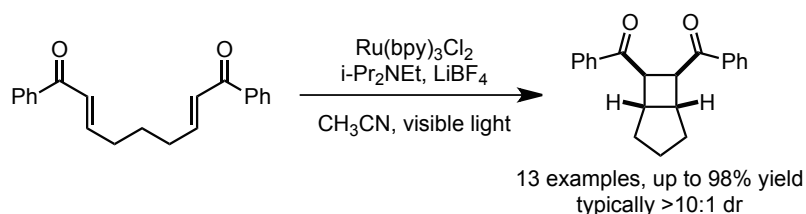
2008: MacMillan, Stephenson and Yoon

The modern era of photoredox catalysis began in 2008 with the submission of two important papers, one by David MacMillan of Princeton and the other by Teshik Yoon of the University of Wisconsin at Madison. These were followed up by important contributions by Corey Stephenson at Boston University (now at the University of Michigan).

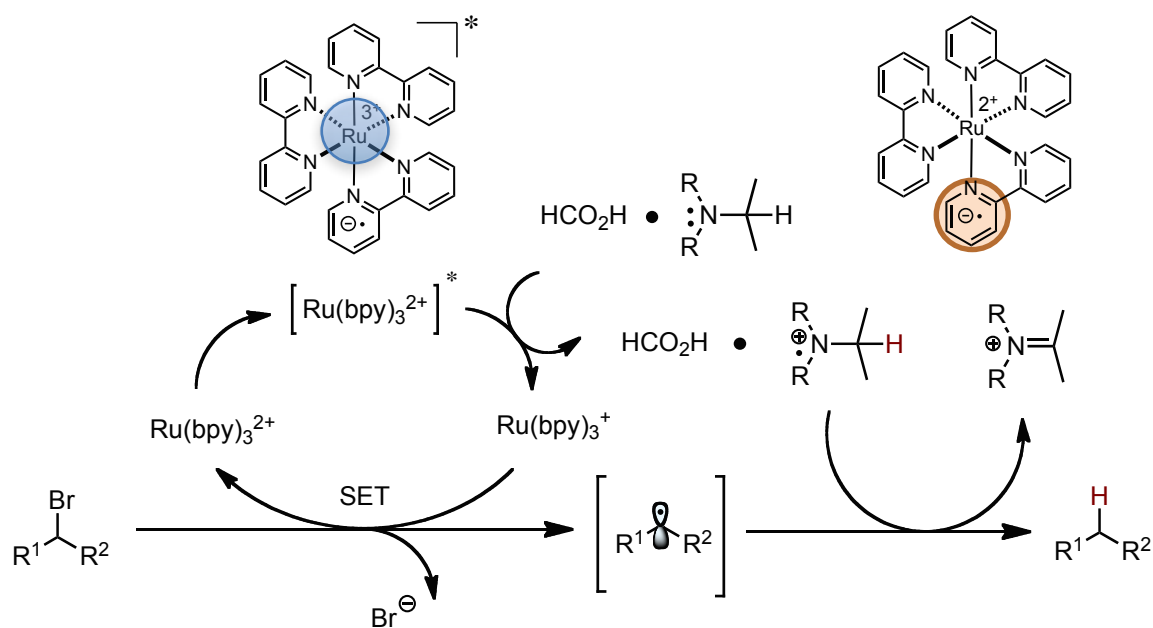
Submitted June 2008: MacMillan and Nicewicz *Science*, **2008**, *322*, 77

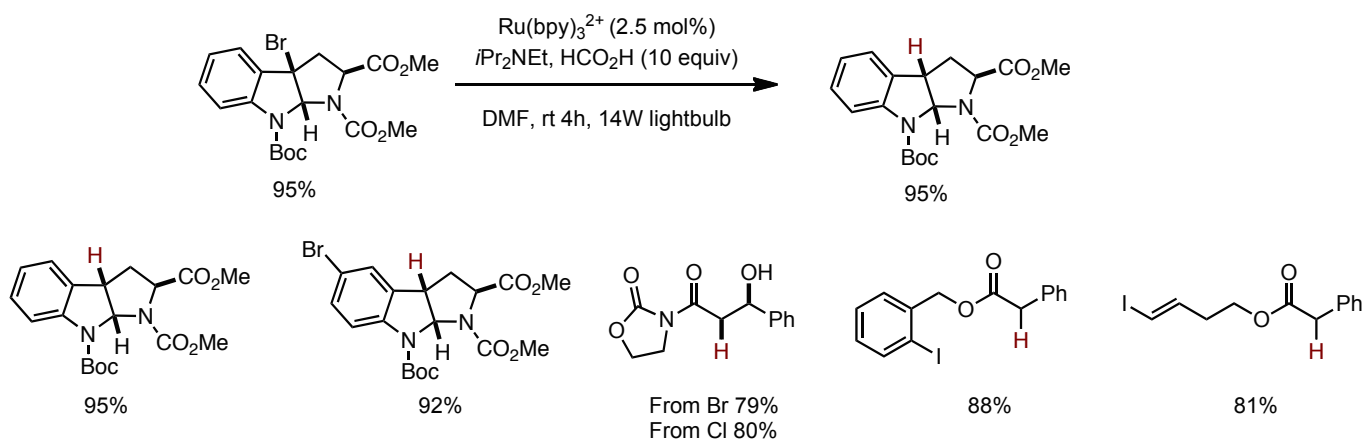


Submitted July 2008: Yoon and Ischay *JACS*, **2008**, *130*, 12886

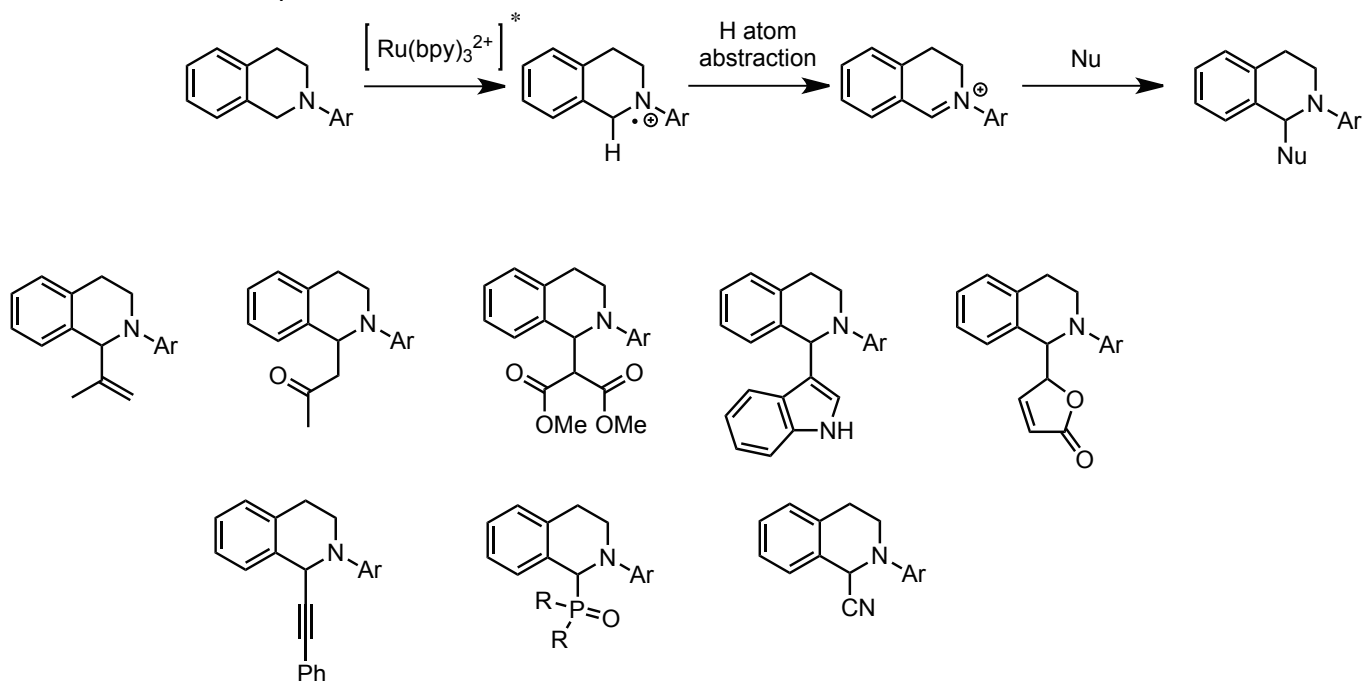


For instance in *JACS* **2009**, *131*, 8756, Stephenson showed how $[\text{Ru}(\text{bpy})_3]^{2+}$ could be used to generate secondary alkyl radicals, which could be quenched in the presence of an amine and formic acid. Note that this catalytic cycle proceeds *via* the reductive quenching pathway. The amine transfers an electron to the excited Ru Complex to form $[\text{Ru}(\text{bpy})_3]^+$ and the nitrogen-centered radical cation, which it itself is converted to the iminium through rapid hydride loss.





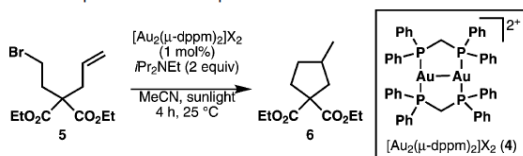
Perhaps the class of reactions where photoredox catalysis has been used the most is to exploit the fact that iminium ions can be generated under mild conditions and can therefore be easily quenched by the presence of an external (or even internal) nucleophile. The example by Stephenson in *Org. Lett.*, **2012**, *14*, 94 illustrates the potential of this reaction class.



4.3 Generality of photoredox catalysts

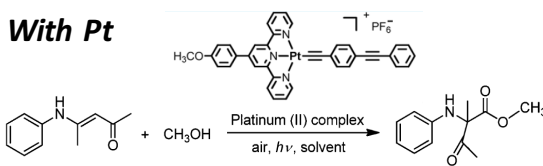
Not only can photoredox catalysis be used for a wide range of different reactions but the type of PRC is not limited only to Ru and Ir complexes. Below are examples with Au, Pt, Re and Cu. These serve to illustrate that many different PRCs can be used.

With Au

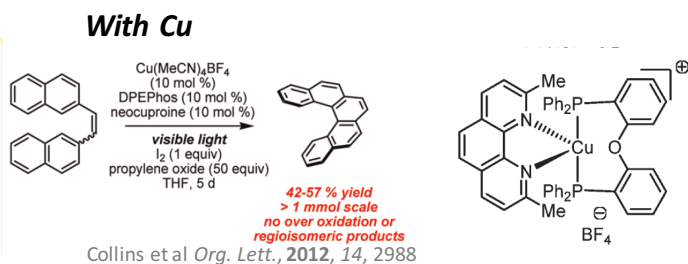
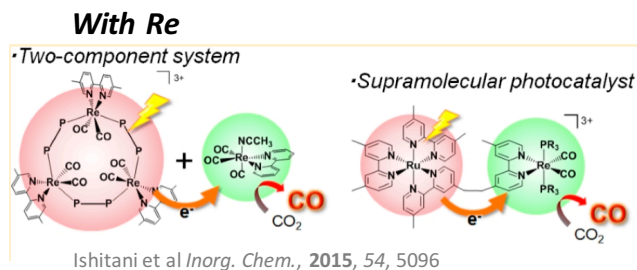


Barriault et al *ACIE*, **2013**, *52*, 13342

With Pt

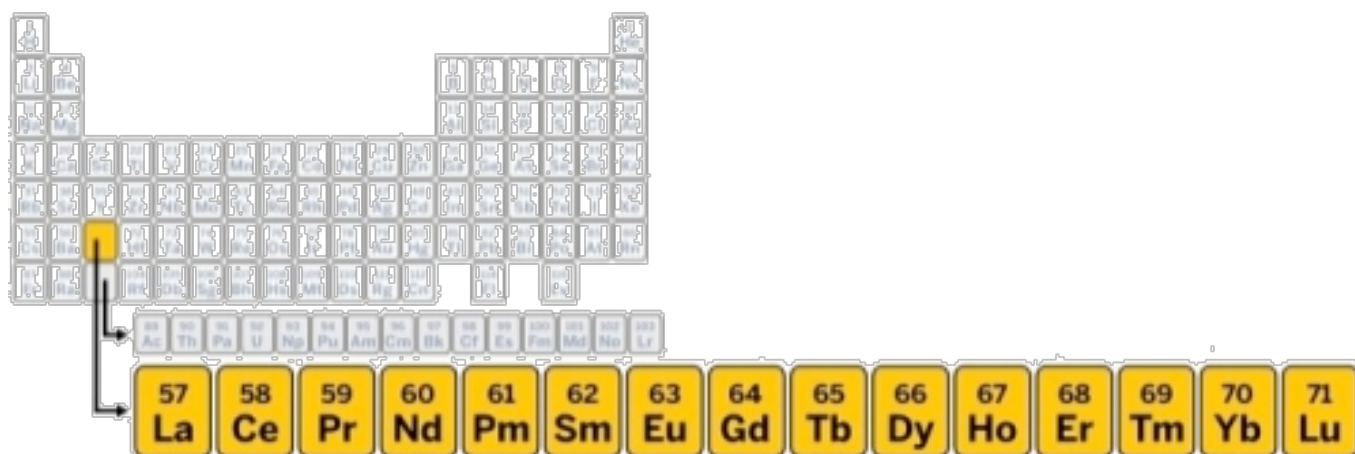


Wu et al *Org. Lett.*, **2014**, *16*, 5968



5 Lanthanoids

The term lanthanoids refers to the elements of the first row of the f-block, ranging from lanthanum to lutetium. The more common term lanthanide has been discouraged by IUPAC as the “ide” normally indicates an anion.



Mixtures of lanthanoids are normally found in minerals such as monazite, basnaesite and xenotime, and their “similar” redox chemistry has made their separation rather difficult.

There exists very small differences in solubility and complexation. Early reports of about 1500 recrystallizations to obtain pure $\text{Tm}(\text{BrO}_3)_3$. No viable purification technique existed before 1955, when different lanthanoids start to appear from fission products of U.

A good number of lanthanoids were first discovered in Ytterby, Sweden (see Table below). In fact, Y, Er, Tb and Yb were all discovered in the same mine.

Johan Gadolin



Per Teodor Cleve

Carl Gustaf Mosander



Year	Element	Origin of name	Discovery	Nationality
1794	Yttrium	Ytterby mine, Sweden	Johan Gadolin	Finnish
1803	Cerium	After the asteroid Ceres	Baron Jons Jakob	Swedish
1839	Lanthanum	From Greek lathano = concealed	Carl Gustav Mosander	Swedish
1843	Erbium	Derived from Ytterby mine, Sweden	Carl Gustav Mosander	Swedish
1878	Terbium	Derived from Ytterby mine, Sweden	Carl Gustav Mosander	Swedish
1878	Ytterbium	Derived from Ytterby mine, Sweden	Jean Charles de Marignac	French
1879	Samarium	After the mineral samarskite	Paul E. Lecoq de Boisbaudran	Swedish
1879	Scandium	After Scandinavia	Lars Fredrik Nilson	Swedish
1879	Holmium	After the Latin for Stockholm	Per Teodor Cleve	Swedish
1879	Thulium	Ancient name for Scandinavia		Swedish
1880	Gadolinium	In honour of Johan Gadolin, a Finnish chemist	Jean de Marignac	Swiss
1885	Praseodymium	From Greek prasios = green, and didymos = twin	Carl Auer von Welsbach	Austrian
1885	Neodymium	From Greek neo = new	Baron Carl Auer von Welsbach	Austrian
1886	Dysprosium	From Greek dys = bad and prositos = approachable	Paul E. Lecoq de Boisbaudran	French
1896	Europium	After Europe	Eugene Demarcay	French
1907	Lutetium	After Lutetia, Latin name for the place where Paris was founded	Georges Urbain, Carl Auer von Welsbach	French and Austrian
1945	Promethium	After Prometheus, in Greek mythology, who brought fire to mankind	Charles DuBois Coryell	American

5.1 Rare-earth elements: Their uses.

Lanthanoids are often termed **rare earths**, which also includes Sc and Y. Sc and Y are considered “part” of the lanthanoid group because they are found in the same ores and share similar chemical properties. China presently controls 97% of the world supply of rare earth ores but as we saw earlier, these elements are actually found abundantly all over the globe. Until recently, they were not so valuable. However, now lanthanoids are found in all sorts of important and useful applications.

 Magnetics Nd Tb, Dy Pr Computer Hard Drives Disk Drive Motors Anti-Lock Brakes Automotive Parts Frictionless Bearings Magnetic Refrigeration Microwave Power Tubes Power Generation Microphones & Speakers Communication Systems MRI CREOs HREOs LREOs	 Phosphors Nd, Eu, Tb, Y Er, Gd Ca, Pr Display phosphors - CRT, LPD, LCD Fluorescent Lighting Medical Imaging Lasers Fibre Optics  Ceramics Nd, Y, Eu Gd, Lu, Dy La, Ce, Pr Capacitors Sensors Colorants Scintillators Refractories	 Metal Alloys Nd, Y La, Ce, Pr NiMH Batteries Fuel Cells Steel Super Alloys Aluminium / Magnesium  Glass & Polishing Nd Gd, Er, Ho La, Ce, Pr Polishing Compounds Pigments & Coatings UV Resistant Glass Photo-Optical Glass X-Ray Imaging	 Catalysts Nd La, Ce, Pr Petroleum Refining Catalytic Converter Fuel Additives Chemical Processing Air Pollution Controls  Defense Nd, Eu, Tb, Dy, Y Lu, Sm Pr, La Satellite Communications Guidance Systems Aircraft Structures Fly-by-Wire Smart Missiles
---	--	---	--

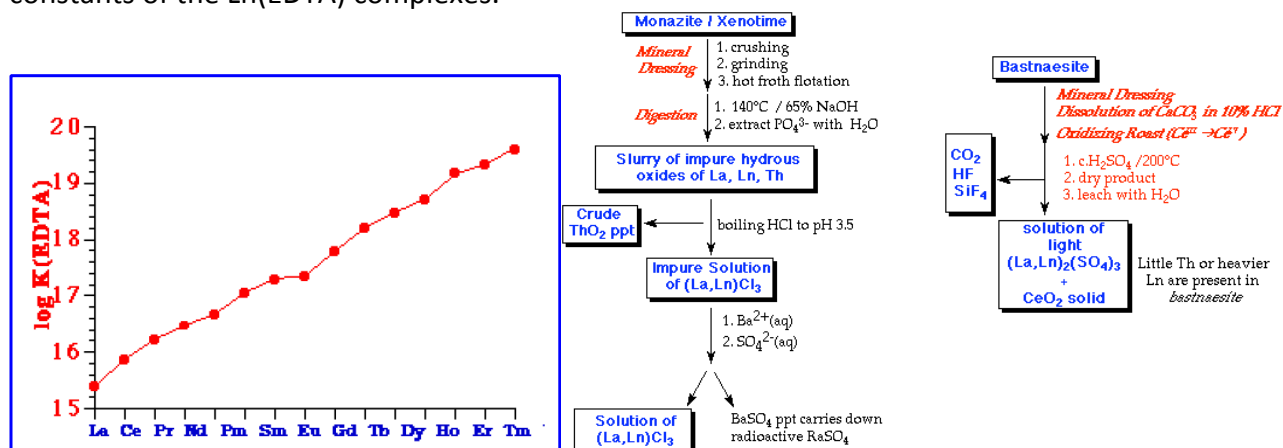
5.2 Isolation and purification of lanthanoids

Cerium & Europium may be extracted Chemically:

Oxidize only Ce to M^{4+} by $HClO$ or $KMnO_4$, then precipitate as CeO_2 or $Ce(IO_3)_4$. On action of Zn/Hg only Eu forms a stable M_{2+} that doesn't reduce H_2O , which can then be isolated by precipitation as $EuSO_4$.

Current Small Scale Lab Separation:

Ion-Exchange Displacement Column. Ln^{3+} (aq) are strongly adsorbed by a cation-exchange resin, add a ligand, typically chelating, e.g., EDTA. The ligand binds most strongly to smallest ion, e.g., the binding constants of the $Ln(EDTA)$ complexes.

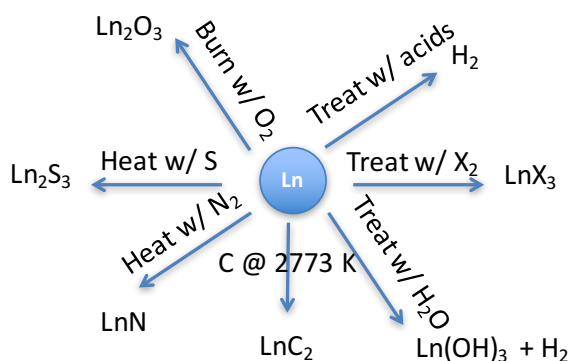


Current Large Scale Industrial Separation:

Solvent Extraction. $\text{Ln}^{3+}(\text{aq})$ is extracted in a continuous counter-current process into a non-polar organic solvent (e.g., kerosene). The solubility of Ln^{3+} in organic solvents increases with its relative atomic mass.

5.3 Properties of lanthanoids

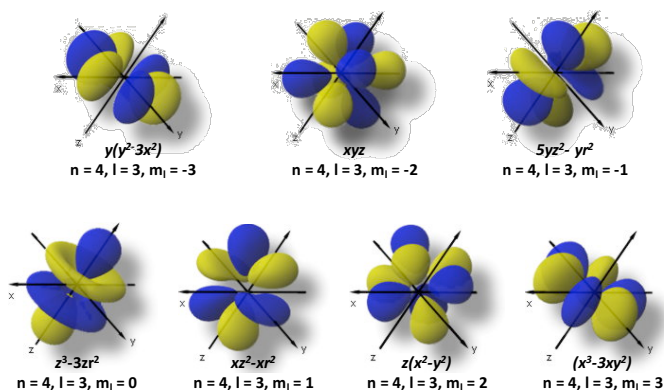
Lanthanoids are silvery white soft metals that tarnish in air rapidly. Their hardness increases across the period (Sm is steel hard). They are good conductors of heat and electricity. Promethium (Pm) is radioactive. They form binaries on heating with most non-metals.



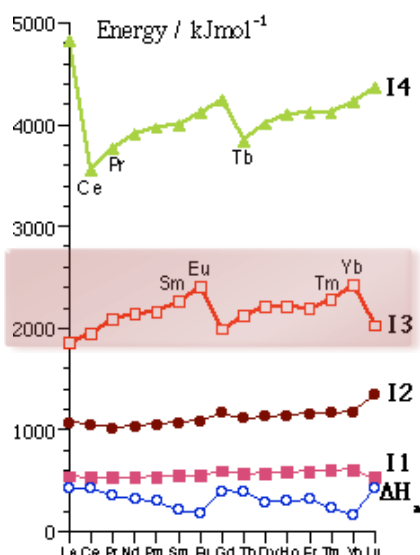
5.3.1 Electronic configuration of lanthanoids

Their electronic configuration has a xenon core. The 6s block is filled. Due to the closeness in energy of the 5d and 4f orbitals, for certain elements an electron may be found in $5d^1$, otherwise the f-shell gets filled up as one moves along the lanthanoid series (see below for electronic configuration of the lanthanoids). There are 7 f-orbitals, which are shown below along with their associated quantum numbers.

	Ln	Ln^{3+}
La	$[\text{Xe}]6s^25d^1$	$[\text{Xe}]4f^0$
Ce	$[\text{Xe}]6s^25d^14f^1$	$[\text{Xe}]4f^1$
Pr	$[\text{Xe}]6s^24f^3$	$[\text{Xe}]4f^2$
Nd	$[\text{Xe}]6s^24f^4$	$[\text{Xe}]4f^3$
Pm	$[\text{Xe}]6s^24f^5$	$[\text{Xe}]4f^4$
Sm	$[\text{Xe}]6s^24f^6$	$[\text{Xe}]4f^5$
Eu	$[\text{Xe}]6s^24f^7$	$[\text{Xe}]4f^6$
Gd	$[\text{Xe}]6s^25d^14f^7$	$[\text{Xe}]4f^7$
Tb	$[\text{Xe}]6s^24f^9$	$[\text{Xe}]4f^8$
Dy	$[\text{Xe}]6s^24f^{10}$	$[\text{Xe}]4f^9$
Ho	$[\text{Xe}]6s^24f^{11}$	$[\text{Xe}]4f^{10}$
Er	$[\text{Xe}]6s^24f^{12}$	$[\text{Xe}]4f^{11}$
Tm	$[\text{Xe}]6s^24f^{13}$	$[\text{Xe}]4f^{12}$
Yb	$[\text{Xe}]6s^24f^{14}$	$[\text{Xe}]4f^{13}$
Lu	$[\text{Xe}]6s^25d^14f^{14}$	$[\text{Xe}]4f^{14}$



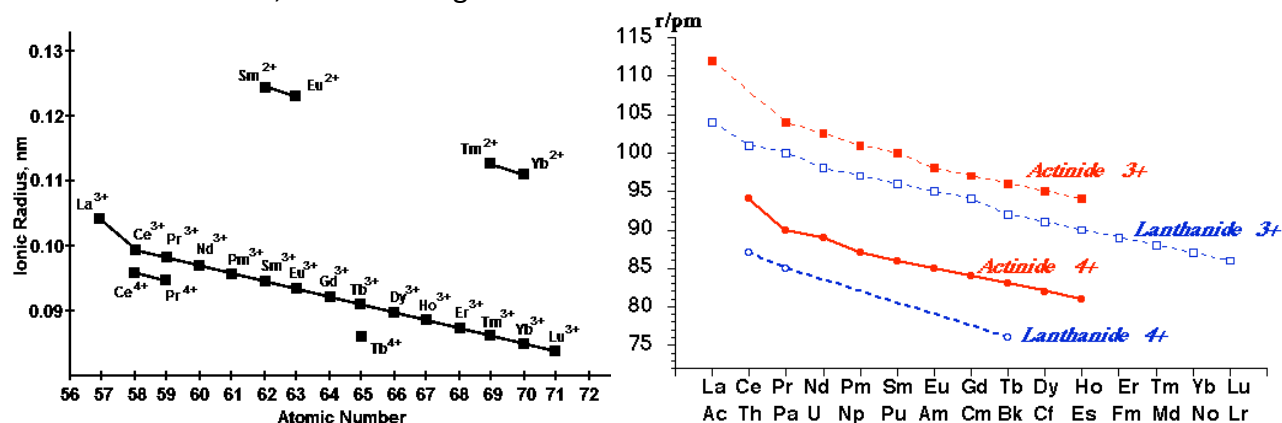
5.3.2 Trends: Oxidation states



The main (and most stable) oxidation state for all the lanthanoid elements is Ln^{3+} . Recent research progress has shown the existence of many Ln^{2+} based compounds, but they tend to oxidize to Ln^{3+} . The lanthanoids have an idealized electronic configuration of $[\text{Xe}]4f^n5d^16s^2$. This means that when they lose 3 electrons, their configuration becomes $[\text{Xe}]4f^n$ and therefore have a closed valence shell and a closed outermost d-sub-shell. Eu^{3+} is the easiest of all the lanthanoids to be reduced to Eu^{2+} . For Ln^{2+} (except for La & Gd) the configuration is likewise $[\text{Xe}]4f^n$. The 4f binding energy is so great that the remaining 4f electrons are regarded as "core-like" (i.e. incapable of modification by chemical means), except Ce. From the figure below, we can see that Sm^{2+} , Eu^{2+} and Yb^{2+} ions in solution are good reducing agents while Ce^{4+} is a good oxidizing agent.

5.3.3.1 Trends: Atomic radii

Along the lanthanoid series, there is a regular decrease in the atomic radii (compare the size of Ho^{3+} being identical to the size of Y^{3+}). This size reduction is caused by the increase in the nuclear charge. The phenomenon is known as the "**lanthanoid contraction**". The effect results from poor shielding of the nuclear charge (nuclear attractive force on electrons) by 4f electrons; the 6s electrons are drawn towards the nucleus, thus resulting in a smaller atomic radius.



5.3.3.2 The nature of the 4f orbitals

What exactly is causing the lanthanoid contraction? Let's think of the nature of the 4f orbitals.

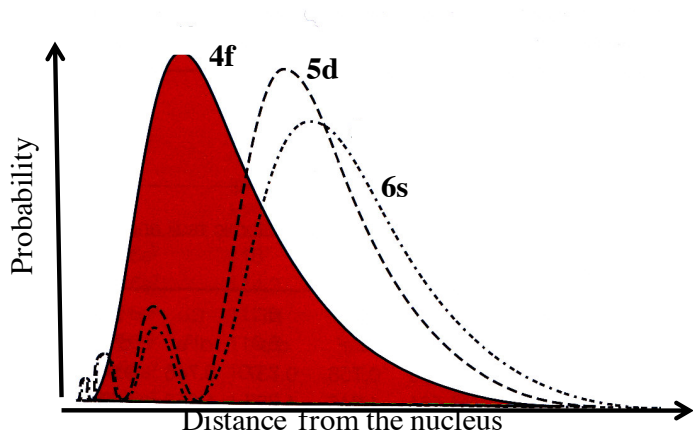
- The 4f orbitals have an inner core nature (5s and 5p orbitals penetrate 4f).
- They are not efficiently shielded from the nuclear charge.
- They are shielded from external ligand fields.
- Relativistic effects, arising from the extremely high velocity with which the electrons travel around nuclei with high nuclear charge, are also responsible for the contraction (see equation below).

$$V_{eff} = -\frac{Z_{eff}}{r} + \frac{l(l+1)}{2r^2} \quad (a.u.)$$

Coulombic & Centrifugal potentials

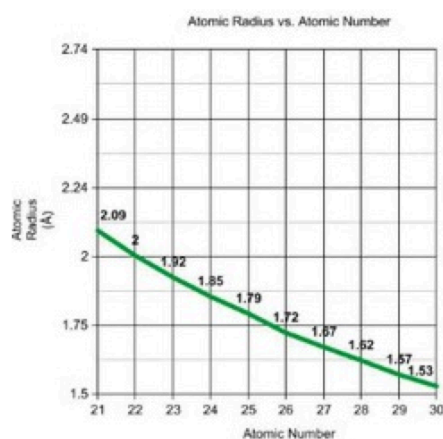
Relativistic effects become apparent when the velocity of the electron is arbitrarily close to the speed of light (137 au) without actually attaining it. At the orbital level, the relativistic effect is apparent in the radial contraction of penetrating s and p shells, expansion of non-penetrating d and f shells, and the spin-orbit splitting of p-, d-, and f-shells.

The evidence of the inner core nature of the 4f orbitals is evidenced in the following properties:

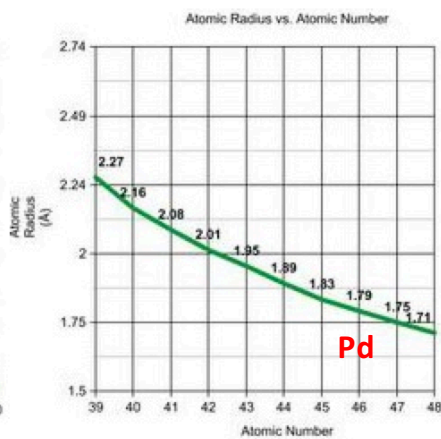


- The metal-to-ligand bonds in Ln^{3+} complexes are essentially ionic.
- Unlike transition metal complexes, there is no directional preference for the donor atoms of the ligands.
- Unlike transition metal complexes, there is no crystalline field effect.
- Ionization of 5d transition metals is higher than 3d and 4d transition metals

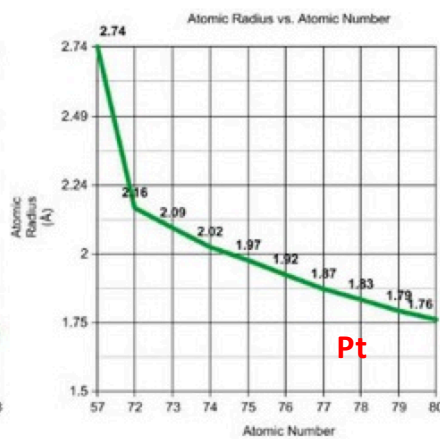
Pd and Pt have about the same atomic radius despite many more electrons present in Pt. This is because these added electrons are in the 4f subshell and don't really contribute to shielding the remaining electrons from the increased size of the nucleus.



Row 1 of Periodic Table D block



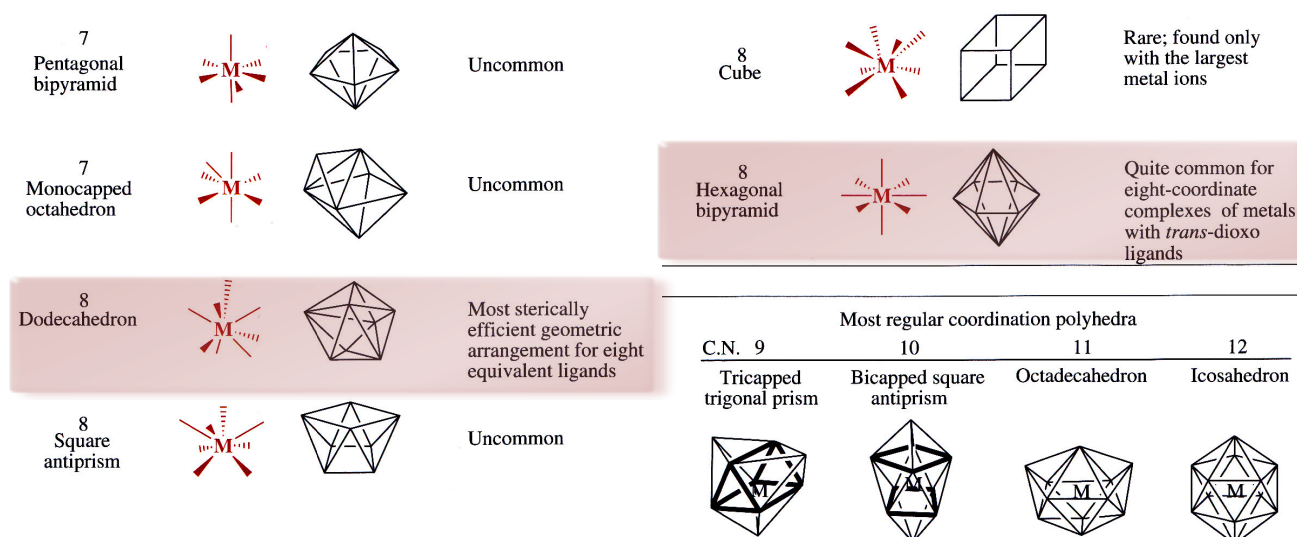
Row 2



Row 3

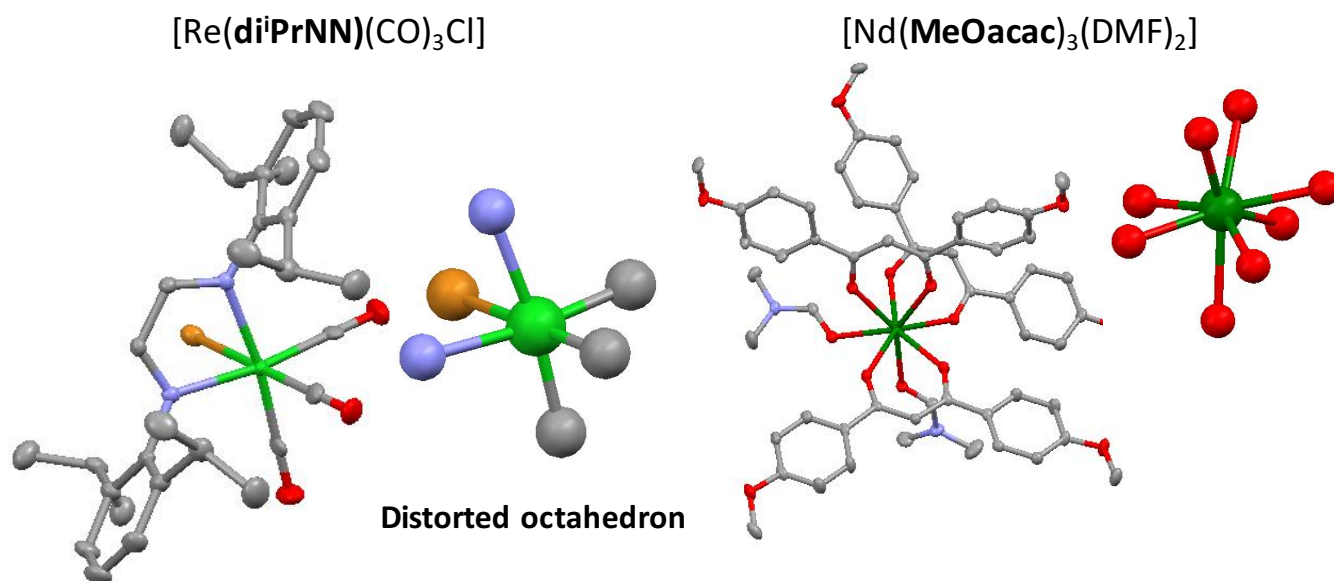
5.3.4 Bonding in f-metal complexes

D-block transition metal complexes favour coordination numbers up until 6. Complexes tend to adopt regular or slightly distorted geometries. Ln^{3+} favour high coordination numbers, generally 8-9 but up until 12. Geometries are less regular. Dodecahedral and hexagonal bipyramidal geometries are the most commonly found amongst lanthanoid complexes.



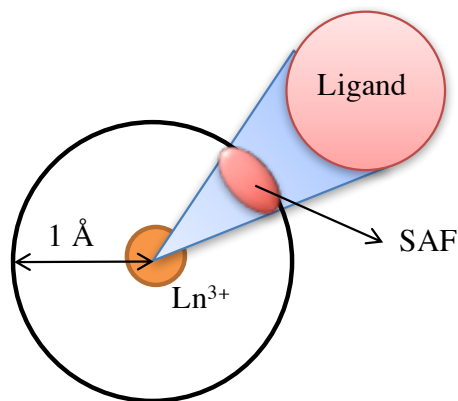
The total number of ligands surrounding the metal centers will depend on the size of the Ln cation and the steric demand of each ligand. When the ligands are not big enough to complete the coordination sphere, more ligands (e.g., solvent) will be added. There is no π -backbonding, no CO species while CpLn complexes are ionic in nature (unlike what is observed for d-block Cp complexes).

Let's compare a Nd^{3+} and a Re^+ coordination compound. The Nd complex is octacoordinated whereas the Re one is hexacoordinated.



It is possible to predict whether a set of ligands around a Ln^{3+} is enough to satisfy the coordination sphere. This is based on the analysis of two empirical parameters, which have been introduced after an analysis of over 150 coordination compounds.

- Solid Angle Factor (SAF)**: it is defined as the proportion of the sphere of radius 100 pm ($= 1 \text{ \AA}$) around the metal ion which is occupied by the ligand.
- Solid Angle Sum (SAS)**: sum of all the SAF of the ligands around the complex.

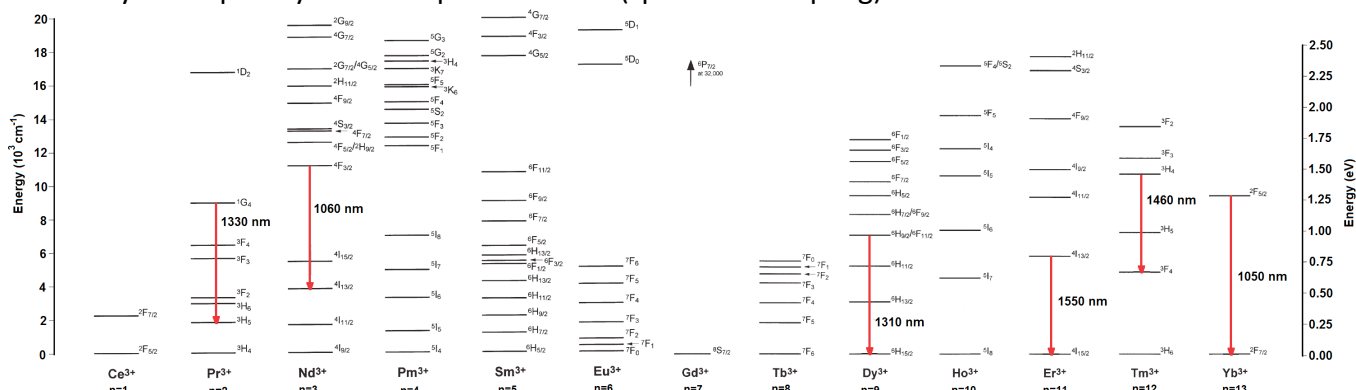


- ✓ Lanthanoid complexes with a **SAS** of around 0.80-0.76 have a complete coordination sphere around the metal center.
- ✓ If the **SAS** is < 0.76 then the complex is likely to have additional ligands (e.g., solvent molecules) added to its coordination sphere.
- ✓ If the **SAS** is > 0.8 , then there is too little space for all the ligands around the metal center and one of them is likely to dissociate.

5.3.5 Crystal field splitting of f-block complexes

In lanthanoid complexes the 4f orbitals are ‘‘inner core’’ and well shielded from the ligand field by the $5s^2$ and $5p^6$ shells. Therefore there is **very limited, sometimes undetectable, crystalline field splitting**.

Analogous f-f transitions exist to d-d transitions of which you are already familiar, but their existence is caused by a completely different phenomenon (spin-orbit coupling).



5.4 A closer look at the electronic configurations of lanthanoids

The electronic configuration specifies the number of electrons in each orbital, however this information is incomplete. Let's consider for example the electronic configuration of Nd^{3+} , $[\text{Xe}]4f^3$. It is clear how all the ‘‘inner core’’ electrons are arranged in the closed shells for the $[\text{Xe}]$ configuration. On the other side, how do 3 electrons arrange in 7 4f orbitals?

Recall that no two electrons may have the same set of quantum numbers [i.e. there is only one way to arrange electrons in a closed shell. Each orbital is filled with two electrons having opposite spin (\uparrow and \downarrow)]. This is none other than the *Pauli exclusion principle*.

In partially filled shells there are multiple ways to arrange all the electrons, for a particular electronic configuration. Each of these different arrangements is termed a **microstate**.

5.4.1 Microstates

A single electronic configuration, with a partially filled shell, is split into different microstates.

Microstates can have different energies because of different degree of electron-electron repulsion. However, different microstates can have the same energy if their electron-electron repulsion is exactly the same.

For lighter elements, when we consider the degree of electron-electron repulsion we have to take into account, in order of contribution:

- The relative orientation of the electron spins
- The relative orientation of the orbital angular momenta

In heavier elements, the spin and angular momenta of individual electrons are strongly coupled together by **spin-orbit coupling**, which becomes the dominant parameter in deciding the relative energies of the microstates.

A microstate is identified by its multiplicity and orbital momenta together, $(2S+1)L$ (called a *spectroscopic term*). The Russell-Saunders coupling scheme is used to identify all the given microstate in an electronic configuration.

L =	0	1	2	3	4	5	6 ...
term	S	P	D	F	G	H	I ...

Microstates are grouped according to their energy to obtain spectroscopically distinguishable energy levels called **terms**.

The multiplicity of a term, i.e., the number of microstates it regroups, is given by $(2S + 1) * (2L + 1)$.

Of all the possible terms, the one with the lowest energy, or **ground term**, is given by Hund's rules and is, by far, the easiest to determine:

- The term with the **greatest spin multiplicity** lies lowest in energy.
- For a given multiplicity, the term with the **greatest value of L** (i.e. lowest orbital multiplicity) lies lowest in energy. *e.g.*, 3F is lower in energy than 3P
- For terms having the same spin multiplicity and the same values of L (*e.g.*, 3P_0 and 3P_1), the level with the **lowest value of J** lies lowest in energy if the sub-level is less than half filled (*e.g.*, f^2) while if the sub-level is more than half filled (*e.g.*, d^8) then the the level with the **highest value of J** lies lowest in energy. If the level is half filled with maximum spin multiplicity (*e.g.*, p^3 with $S = 3/2$), L must be zero and $J = S$

How does one construct a table of microstates? The following set of rules illustrates how this can be done:

1. Write down the electron configuration (*e.g.*, d^2)
2. Ignore closed shell electron configurations (*e.g.*, ns^2 , np^6 , nd^{10}) as these will always give a 1S_0 term.
3. Determine the number of microstates: for x electrons in a sub-level of $(2l+1)$ orbitals, this is given by:

$$\frac{\{2(2l + 1)\}!}{x!\{2(2l + 1) - x\}!}$$

4. Tabulate microstates by m_l and m_s , and sum to give M_L and M_S on each row. Check that the number of microstates in the table is the same as that expected from rule 3.
5. Collect the microstates into groups based on values of M_L .

For example,

for **hydrogen, Z=1:**

$m_l = 0$	$M_L = \sum m_l$	$M_S = \sum m_s$	
↑	0	+1/2	} L = 0, S = 1/2
↓	0	-1/2	

$$\text{Number of microstates} = \frac{\{2(2l + 1)\}!}{x!\{2(2l + 1) - x\}!} = \frac{2!}{1! \cdot 1!} = 2$$

${}^2S_{1/2}$

for **boron Z=5:**

$m_l = +1$	$m_l = 0$	$m_l = -1$	$M_L = \sum m_l$	$M_S = \sum m_s$	
↑			+1	+1/2	} L = 1, S = 1/2
	↑		0	+1/2	
		↑	-1	+1/2	
		↓	-1	-1/2	} L = 1, S = 1/2
	↓		0	-1/2	
↓			+1	-1/2	

$$\text{Number of microstates} = \frac{\{2(2l + 1)\}!}{x!\{2(2l + 1) - x\}!} = \frac{6!}{1! \times 5!} = 6$$

Only the $2p^1$ configuration contributes, but there are 3 distinct p orbitals.

for a **d^2 high spin metal such as Ti^{II} :**

$$\text{Number of microstates} = \frac{\{2(2l + 1)\}!}{x!\{2(2l + 1) - x\}!} = \frac{10!}{2! \times 8!} = 45$$

$m_l = +2$	$m_l = +1$	$m_l = 0$	$m_l = -1$	$m_l = -2$	M_L	
↑	↑				+3	} ${}^3F (L = 3)$
↑		↑			+2	
↑			↑		+1	
↑				↑	0	
	↑			↑	-1	
		↑		↑	-2	
			↑	↑	-3	
	↑	↑			+1	} ${}^3P (L = 1)$
	↑		↑		0	
		↑	↑		-1	

Table 21.9 A shorthand table of microstates for a d^2 configuration; only a high-spin case (weak field limit) is considered, and each electron has $m_s = +\frac{1}{2}$. The microstates are grouped so as to show the derivation of the 3F and 3P terms. Table 21.7 provides the complete table of microstates for a d^2 ion.

Housecroft and Sharpe, *Inorganic Chemistry*, 3rd Edition © Pearson Education Limited 2008

for Eu^{III} :

The electronic configuration is $4f^6$. Therefore, the multiplicity of the term is $(2S+1)(2L+1) = 49$.

The largest multiplicity is obtained when each electron is associated with a unique $4f$ wavefunction: $S = 6 * \frac{1}{2} = 3$; therefore, $(2S + 1) = 7$.

To obtain the largest orbital multiplicity, these electrons have to be related with wavefunctions having the largest m_l values, i.e., 3, 2, 1, 0, -1, and -2; the sum, $M_l = 3$

Thus, $L = 3$ and the term is **F**

The ground term is a spin septet, 7F with overall multiplicity $7*7 = 49$.

5.4.2 Spin-orbit coupling

The terms ${}^{(2S+1)}L$ consider spin-orbit coupling to be negligible. These terms best describe lighter elements, including first row transition metal elements. For heavier elements the terms become ${}^{(2S+1)}L_J$, where J is the spin-orbit coupling.

$J = (L + S), (L + S - 1), \dots, |L - S|$, these values can be 0, 1, 2 or $\frac{1}{2}, \frac{3}{2}, \frac{5}{2} \dots$

with the **Total Angular Momentum** = $\frac{(\sqrt{J(J+1)})\hbar}{2\pi}$

There are $(2S+1)$ possible values of J for $S < L$ and $(2L+1)$ possible values of J for $L < S$.

M_J denotes the component of the total angular momentum along the z-axis, with $M_J = J, J-1, \dots, -(J-1), -J$

For a given ${}^{(2S+1)}L_J$ term, **if the shell is less than half filled, then the lowest J lies lower in energy. If the shell is more than half filled, then the highest J lies lowest in energy.**

Let's consider a $4d^2$ system

So $n = 4$, $l = 0$ to 3 ,

$m_l = -3$ to 3 and

$m_s = -1/2, +1/2$

One can observe from the figure to the right how taking into account spin-orbit coupling further splits the 3P and 3F microstates into three additional substates, related by their J value.

Let's now determine the ground term of Sm^{3+} .

Its electronic configuration is $[Xe]4f^5$.

Draw the 7 $4f$ orbitals with their m_l values

+3	+2	+1	0	-1	-2	-3
----	----	----	---	----	----	----

Place the 5 electrons. Start from the highest m_l and place 1 electron for each orbitals, all with the same spin.

+3 ↑	+2 ↑	+1 ↑	0 ↑	-1 ↑	-2	-3
------	------	------	-----	------	----	----

$$S = \frac{1}{2} + \frac{1}{2} + \frac{1}{2} + \frac{1}{2} + \frac{1}{2} = \frac{5}{2}$$

$$\text{Multiplicity} = 2S + 1 = 6$$

Now determine S and the spin multiplicity:

$$L = 3 + 2 + 1 + 0 - 1 = 5$$

term = H

Then determine L :

The ground term is a 6H , **Recall that the term is:** $(2S+1)L_J$

Let's now include spin-orbit coupling to the 6H_J . Because the shell is less than half filled, then the lowest value of J is the ground term, which is: $^6H_{5/2}$. Recall that:

$$J = |L + S|, |L + S| - 1, \dots, |L - S|$$

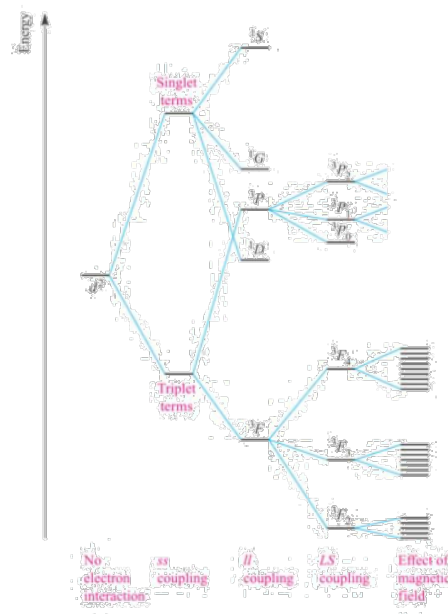
$$J = 5 + 5/2, 5 + 5/2 - 1, \dots, 5 - 5/2$$

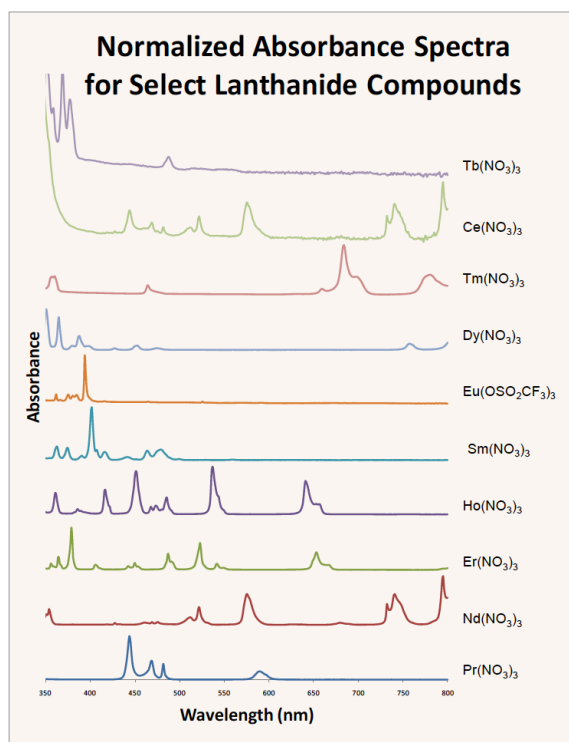
$$J = 15/2, 13/2, \dots, 5/2$$

5.5 Absorption properties of lanthanoids

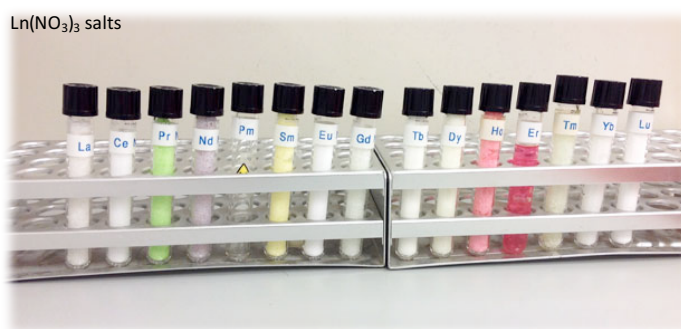
As a consequence of the Laporte forbidden nature of $4f$ transitions, direct absorption of Ln^{III} ions is very weak ($\epsilon < 10 \text{ M}^{-1} \text{ cm}^{-1}$). La^{3+} and Lu^{3+} have no colour as they either have no electrons in or possess a fully filled $4f$ subshell, respectively.

Ligand field effects are very small. Absorption bands are narrow and are virtually independent of environment due to their being essentially no crystal/ligand field effects on the lanthanoid $4f$ orbitals.





Ion	Unpaired Electrons	Color	Ion	Unpaired Electrons	Color
La ³⁺	0	Colorless	Tb ³⁺	6	Pale Pink
Ce ³⁺	1	Colorless	Dy ³⁺	5	Yellow
Pr ³⁺	2	Green	Ho ³⁺	4	Pink; yellow
Nd ³⁺	3	Reddish	Er ³⁺	3	Reddish
Pm ³⁺	4	Pink; yellow	Tm ³⁺	2	Green
Sm ³⁺	5	Yellow	Yb ³⁺	1	Colorless
Eu ³⁺	6	Pale Pink	Lu ³⁺	0	Colorless
Gd ³⁺	7	Colorless			



Ce^{III} and Tb^{III} have high intensity bands in the UV due to $4f^n \rightarrow 4f^{n-1} 5d^1$ transitions. i.e. these are f-d transitions and therefore not orbitally forbidden (respect Laporte selection rule)

5.6 Magnetism properties of lanthanoids

There are two main kinds of magnetic behaviour that can be observed when an atom, ion or molecule is placed in an applied magnetic field.

- **Diamagnetism:** circulation of electron pairs induced by the presence of an external field, which produces an induced magnetic moment, which opposes the external field.
- **Paramagnetism:** caused by unpaired electrons, which produce an induced magnetic field aligned with the external one.

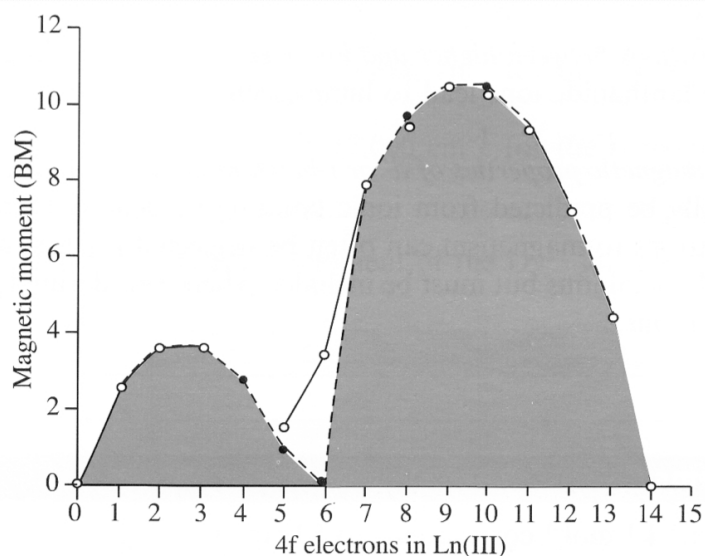
Magnetic properties have spin & orbit contributions (contrast to "spin-only" of transition metals). Magnetic moments of Ln³⁺ ions are generally well described from the coupling of spin and orbital angular momenta - Russell-Saunders Coupling Scheme. Their magnetism is essentially independent of environment. For elements with significant spin-orbit coupling contribution (SOC $\sim 1000 \text{ cm}^{-1}$), such as Ln the **Landé formula** is used to estimate the magnetic moment μ_J of atoms or ions in Bohr magnetons (BM):

$$\mu_J = g_J [J(J+1)]^{1/2}$$

$$g_J = \frac{3}{2} + \frac{[S(S+1) - L(L+1)]}{2J(J+1)}$$

Moments of Sm^{III} and Eu^{III} are altered from the Landé expression by temperature-dependent population of low-lying excited J-state(s).

Ln	$g_J\sqrt{J(J+1)}$	Observed μ_{eff}/μ_B
La	0	0
Ce	2.54	2.3 - 2.5
Pr	3.58	3.4 - 3.6
Nd	3.62	3.5 - 3.6
Pm	2.68	-
Sm	0.85	1.4 - 1.7
Eu	0	3.3 - 3.5
Gd	7.94	7.9 - 8.0
Tb	9.72	9.5 - 9.8
Dy	10.65	10.4 - 10.6
Ho	10.6	10.4 - 10.7
Er	9.58	9.4 - 9.6
Tm	7.56	7.1 - 7.6
Yb	4.54	4.3 - 4.9
Lu	0	0



Solid line, experimental measurements; broken line, calculated values

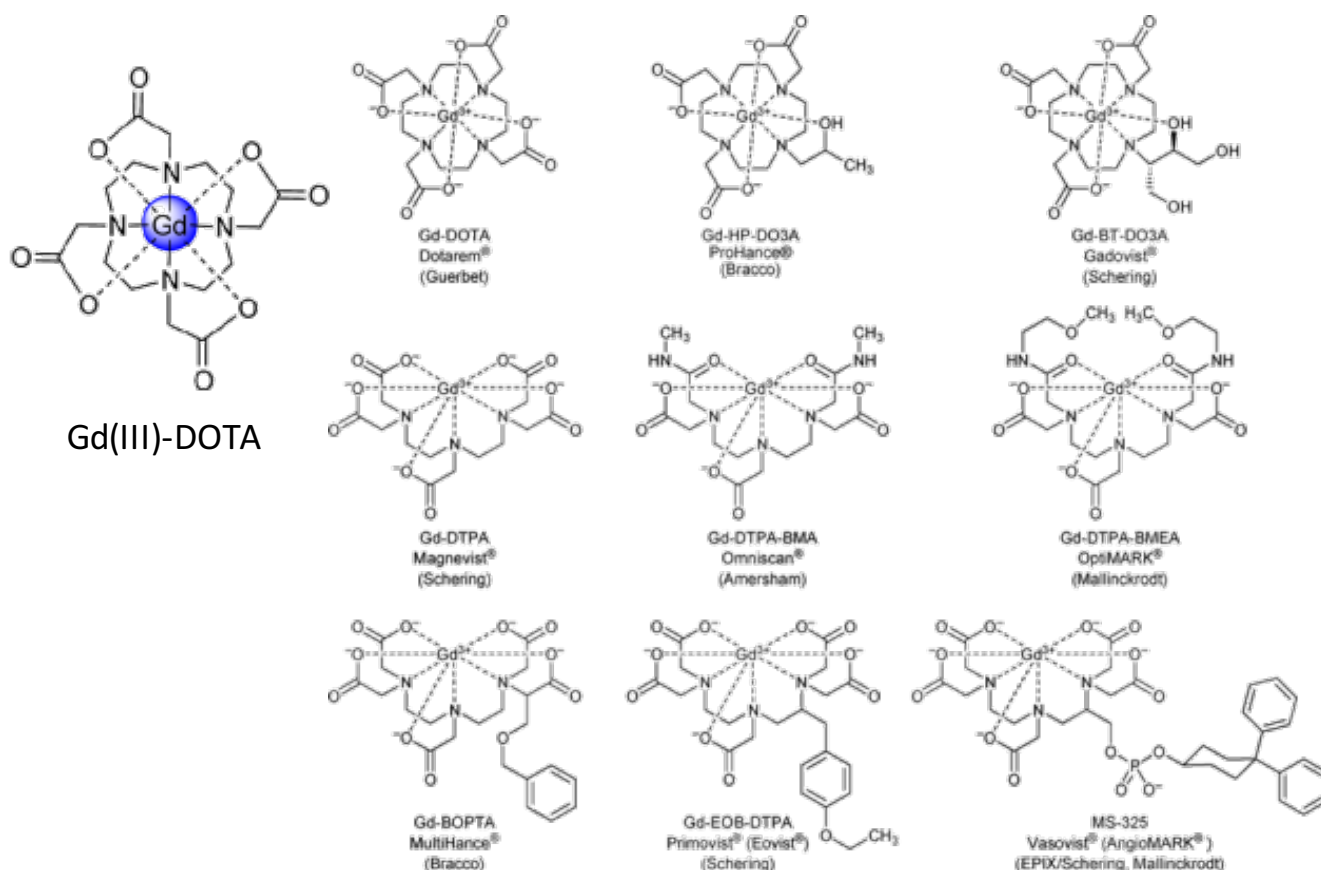
All Ln^{3+} are paramagnetic except for f^0 , f^1 (La^{3+} and Ce^{3+}) and f^{13} , f^{14} (Yb^{3+} and Lu^{3+}) types. Paramagnetism is a maximum with Nd^{3+} .

5.6.1 MRI Imaging and contrast reagents

Magnetic resonance imaging (MRI) is one of the most powerful diagnostic tools in medicine. An MR image is acquired by inserting a specimen within an external magnetic field and applying a short RF pulse, thereby exciting the water protons. Over time, the water protons relax to equilibrium where this process occurs at different rates within different types of environments such as cells or tissue. Tissues with faster relaxation rates provide greater signal intensity.

To improve the sensitivity of MRI, Gd^{III} -based contrast agents are employed to differentiate between regions of interest that are histologically distinct, but magnetically similar. The reason Gd^{III} is used is that as a $4f^7$ ion its spin is $S=7/2$, which is very high.

Below are a series of Gd^{III} contrast reagents. Note the similarity in structural design.



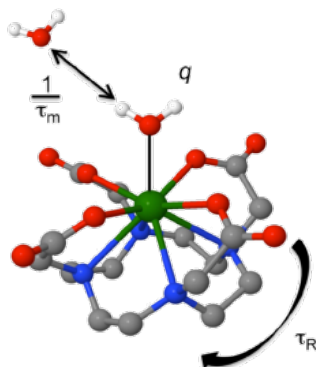
The magnetic field generated by the unpaired electrons of Gd^{III} interacts with water molecules to increase their relaxation rate, improving signal intensity.

$$\frac{1}{T_{1,obs}} = \frac{1}{T_{1,d}} + \frac{1}{T_{1,p}} \qquad \frac{1}{T_{1,obs}} = \frac{1}{T_{1,d}} + r_1[Gd]$$

where $T_{1,d}$ is the diamagnetic term, $T_{1,p}$ is the paramagnetic term and r_1 is the relaxivity.

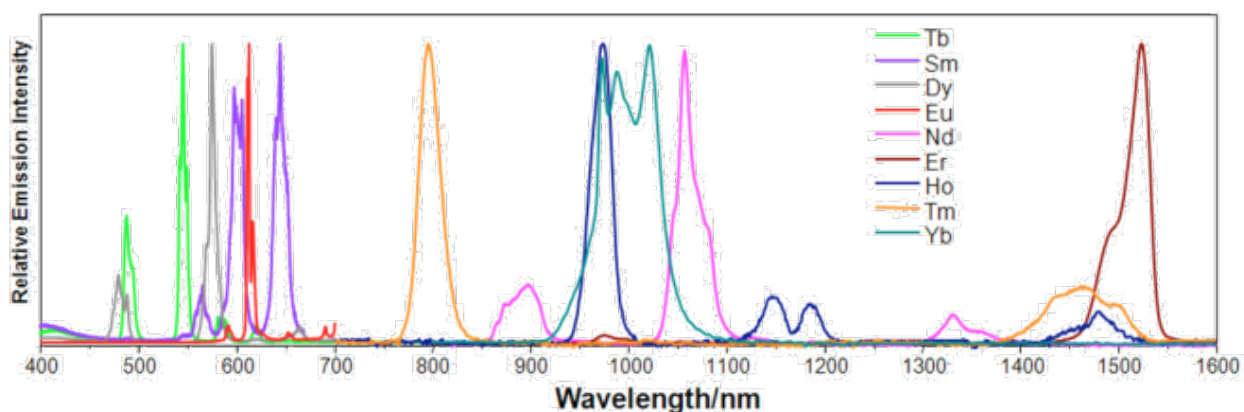
Three parameters influence r_1 :

1. q : the number of water molecules directly bound to Gd^{III}
 - $\uparrow q$ leads to $\uparrow r_1$
 - can be achieved by decreasing the coordination number around Gd^{III} , but this will result in a loss of kinetic stability of the complex and an increase in toxicity
2. τ_m : the inverse of the exchange rate of the bound water with the bulk solvent
 - $\downarrow \tau_m$ leads to $\uparrow r_1$ but can't be too rapid or full relaxation can't occur
 - ideal values of τ_m : 10–20 ns for a 1-3 T magnet
3. τ_R : the rotational correlation time of the complex (how fast it tumbles in solution)
 - $\uparrow \tau_R$ leads to $\uparrow r_1$
 - need large molecular weight contrast reagents to decrease tumbling rate



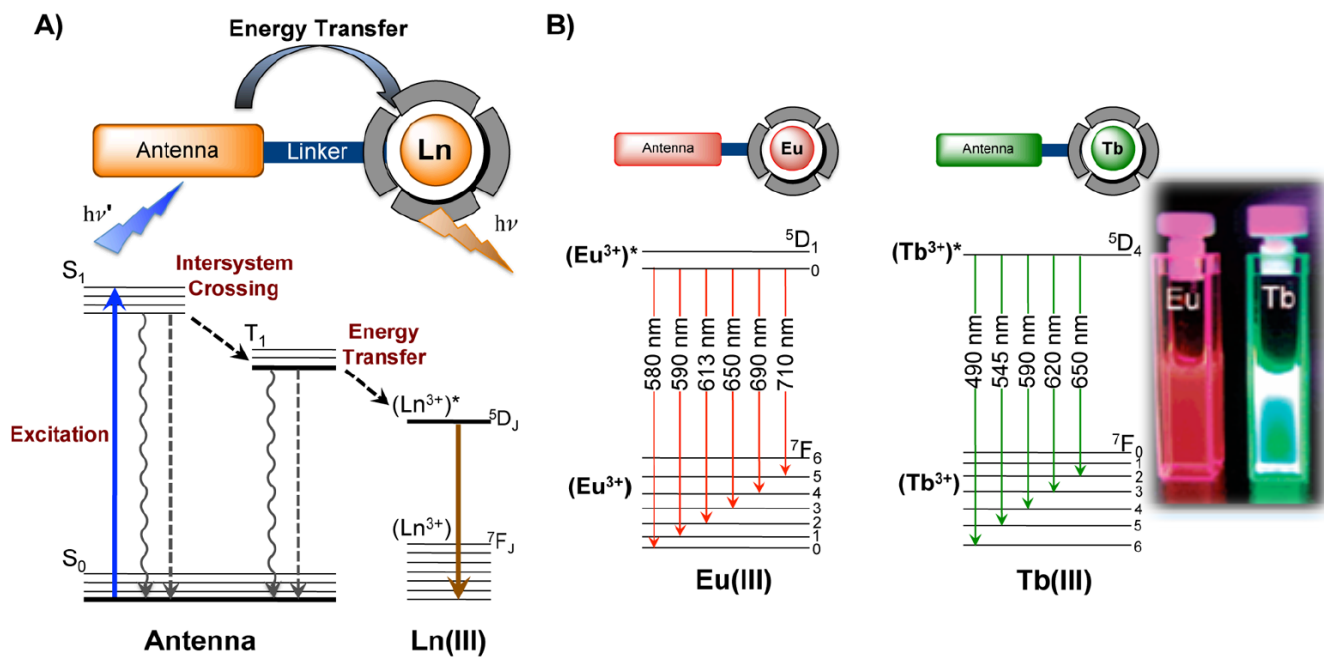
5.7 Emission properties of lanthanoids

Luminescence from lanthanoid complexes ranges from Vis to IR emission. Emission originates from $f \rightarrow f$ transitions. Each ion has a characteristic emission, with narrow emission bands with no vibronic structure (see below). Typically there have long emission lifetimes, τ_e , show no oxygen sensitivity or photo bleaching. These properties of luminescent lanthanoid complexes have generated interest in their use in counterfeit protection of currency (used in Euro bills), electroluminescent devices and bioimaging. The long emission lifetimes in particular mitigate issues of autofluorescence, which itself occurs over very short nanosecond time scales.

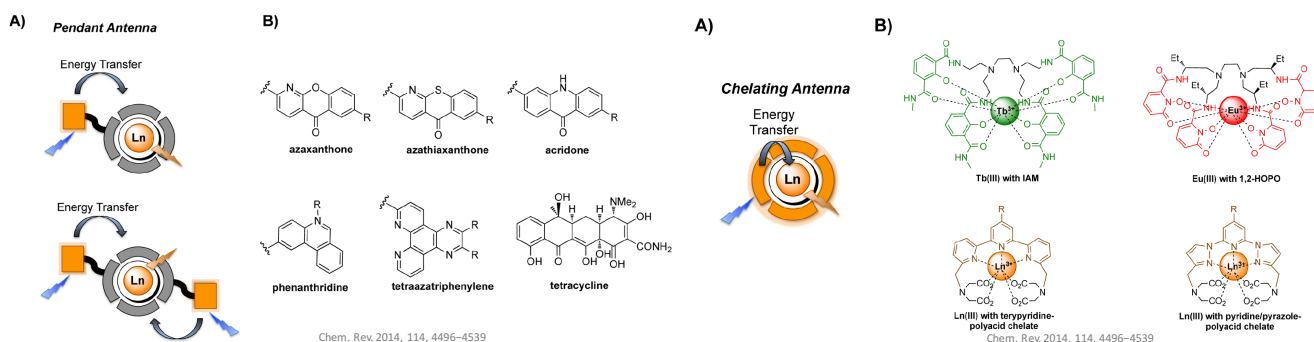


As lanthanoids are so poorly absorptive, Direct excitation of Ln^{3+} ions is inefficient (electronic transition between $f-f$ orbitals – Laporte forbidden). If an organic chromophore is placed in the vicinity of a Ln^{3+} , energy can be transferred from the excited state of the organic molecules to the Ln^{3+} , with consequent emission from the metal center. This process is called **lanthanoid sensitization** and the use of organic chromophores is commonly known as the **antenna effect**. For more details see: *Chem. Rev.* **2014**, *114*, 4496–4539.

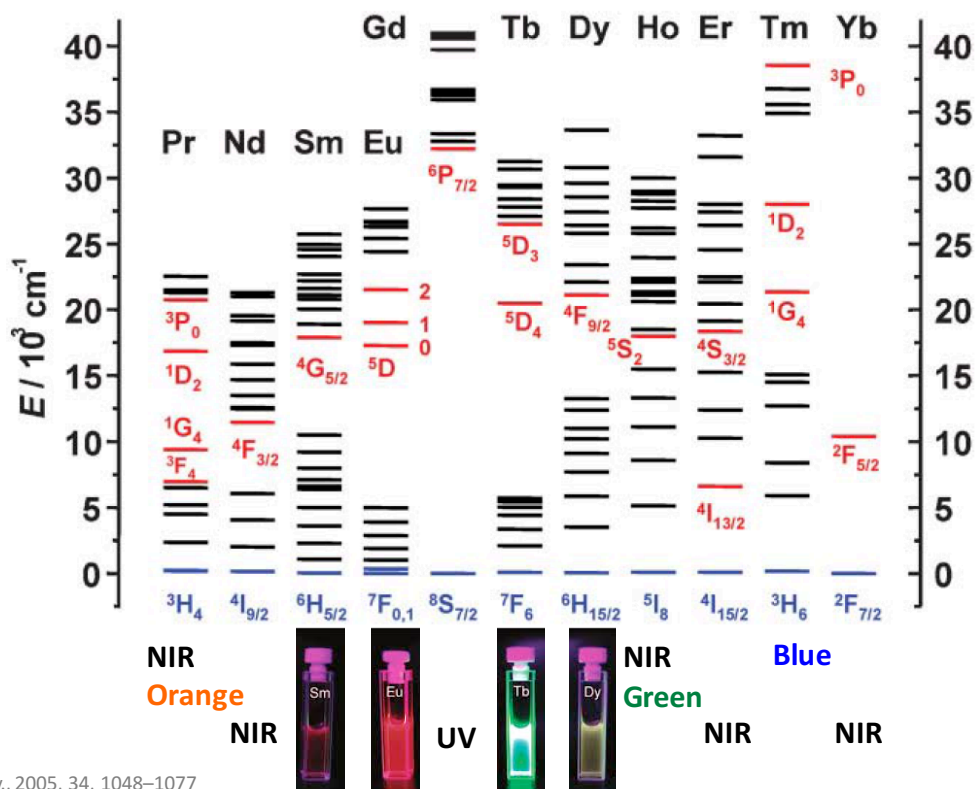
The emission profile of the Ln complex (i.e. the number of emission lines observed) is related to the spin-orbit coupling term. So for Eu^{III} where the ground state term is 7F_1 , there are 7 J values ($L = 3$ and $S = 3$) and therefore 7 possible emission lines (six of which are experimentally distinguishable – see below).



Generally speaking, the organic chromophore can either directly be bound to the lanthanoid metal as part of the ligand or can be covalently tethered to the ligand scaffold. See below for examples of each.



Depending on the lanthanoid, emission can range from UV to NIR. Below is an energy diagram showing in red the main luminescent level and in blue the fundamental level.



Chem. Soc. Rev., 2005, 34, 1048–1077

To summarize:

- ✓ Luminescence is radiative decay following electronic excitation.
- ✓ Electronic transitions are allowed if $\Delta S = 0$ and $\Delta l \neq 0$.
- ✓ Fluorescence is radiative decay characterized by $\Delta S = 0$ and short excited state lifetime (e.g. $^5H_3 \rightarrow ^5D_7$).
- ✓ Phosphorescence is radiative decay characterized by $\Delta S \neq 0$ and long excited state lifetime (e.g. $^5H_3 \rightarrow ^4D_7$).
- ✓ Lanthanoids are characterized by sharp emission lines, which are independent from the surrounding ligands.
- ✓ Direct excitation of lanthanoid cations is **Laporte forbidden**, hence chromophores are used to activate the lanthanoid excited states via energy transfer (**antenna effect**).

5.8 Overview of the properties of lanthanoids

Pre-Transition Metals	Lanthanides	Transition Metals
Essentially Monovalent - show Group (n+) oxidation state	Essentially Monovalent (+3). +2/+4 for certain configs	Show Variable Valence (extensive redox chemistry) control by environment - ligands, pH etc... Size changes of M^{n+} less marked.
Periodic trends dominated by (effective nuclear) charge at noble gas config (i.e. on group valence).	Lanthanide Contraction of Ln^{3+} .	
Similar Properties for a given group (differentiated by size). widespread on earth.	Similar Properties (differentiated by size). common mineralogy	Substantial Gradation in Properties. diverse mineralogy
No Ligand Field Effects.	Insignificant Ligand Field Effects.	Substantial Ligand Field Effects.
Always 'hard' (O, Hal, N donors) (preferably -vely charged)	Always 'hard' (O, X, N donors) (preferably -vely charged)	Later (increasingly from Fe-Cu)/heavier metals may show a 'soft' side.
'Ionic' or 'Covalent' Organometallics	'Ionic' Organometallics.	'Covalent' Organometallics.
No Ligand Effects.	Paucity of Ligand Effects.	π -Acceptor Ligands - Extensive Chemistry.
Poor Coordination Properties (C.N. determined by size).	High Coordination Numbers (C.N. determined by size).	Extensive Coordination C.N. = 6 is typical maximum (but many exceptions).
Flexibility in Geometry.	Flexibility in Geometry.	Fixed (by Ligand Field effects) Geometries.
No Magnetism from the metal ions - noble gas configurations of ions	Free Ion-like Magnetism ground state magnetism	Orbital Magnetism 'Quenched' by Ligand Fields. excited J-states populated.
'Ionic' compound formulations \rightarrow large HOMO-LUMO gaps \rightarrow UV CT spectra	Weak, Narrow Optical Spectra. Forbidden, unassisted transitions.	Stronger, Broader Optical Spectra. Forbidden transitions. Vibronically-assisted.

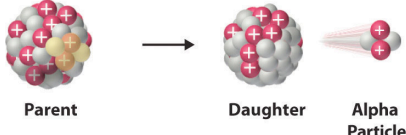
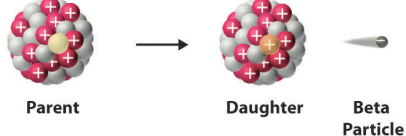
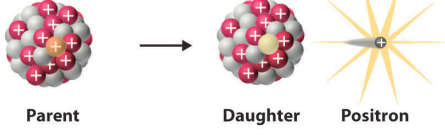
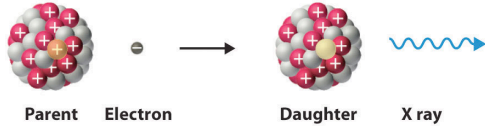
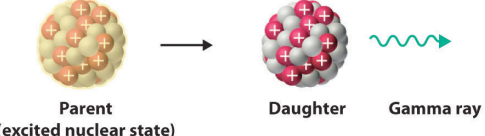
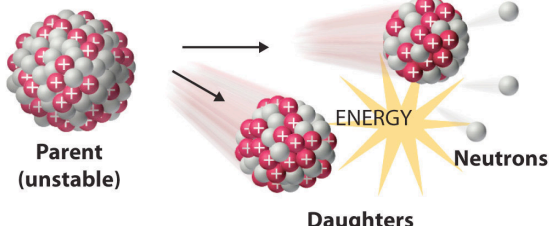
6 Actinoids

Actinoids are the elements of the 5f block of the periodic table. All isotopes are radioactive, with only ^{232}Th , ^{235}U , ^{238}U and ^{244}Pu having long $t_{1/2}$. Only Ac, Pa, Th and U occur naturally ($Z < 93$) – the latter two are both more abundant in the Earth's crust than Sn. All the other actinoids must be made by nuclear processes.

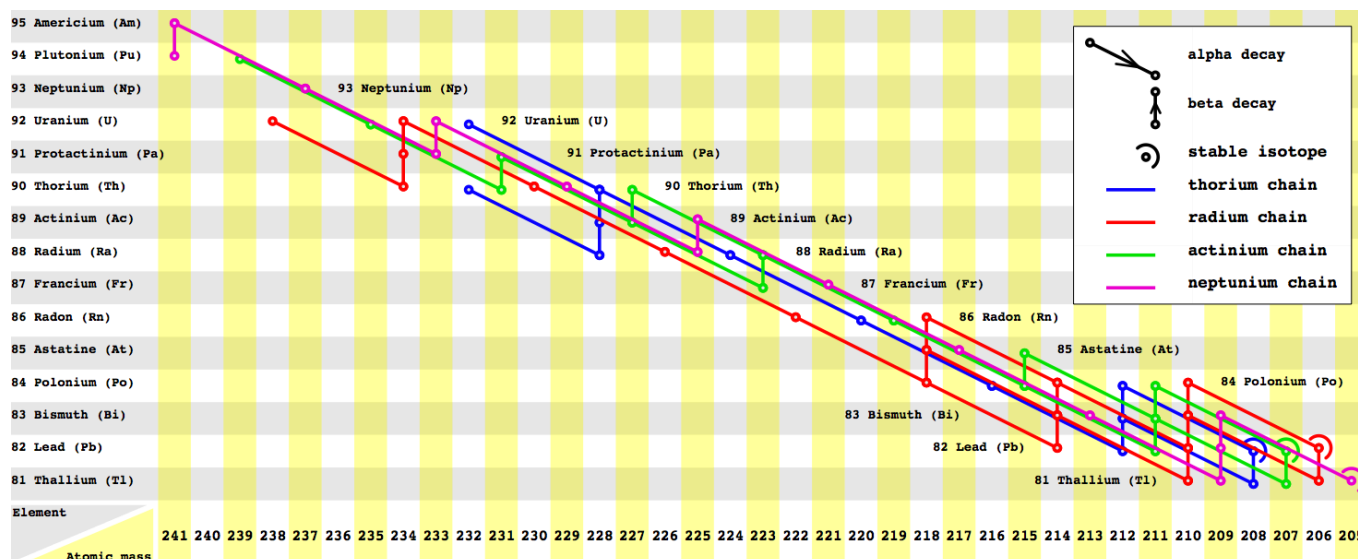
ACTINIDES													
89 Ac (227)													
90 Th (232)	91 Pa (231)	92 U (238)	93 Np (237)	94 Pu (244)	95 Am (243)	96 Cm (247)	97 Bk (247)	98 Cf (251)	99 Es (252)	100 Fm (257)	101 Md (258)	102 No (259)	103 Lr (260)

6.1 Radioactive decay modes and decay chains in actinoids

Given the important property of radioactivity in actinoids, it is important to understand that there are at least six important decay modes that are operational. These are shown below. Importantly, only α decay results in a change in the atomic mass, A, (of four amu).

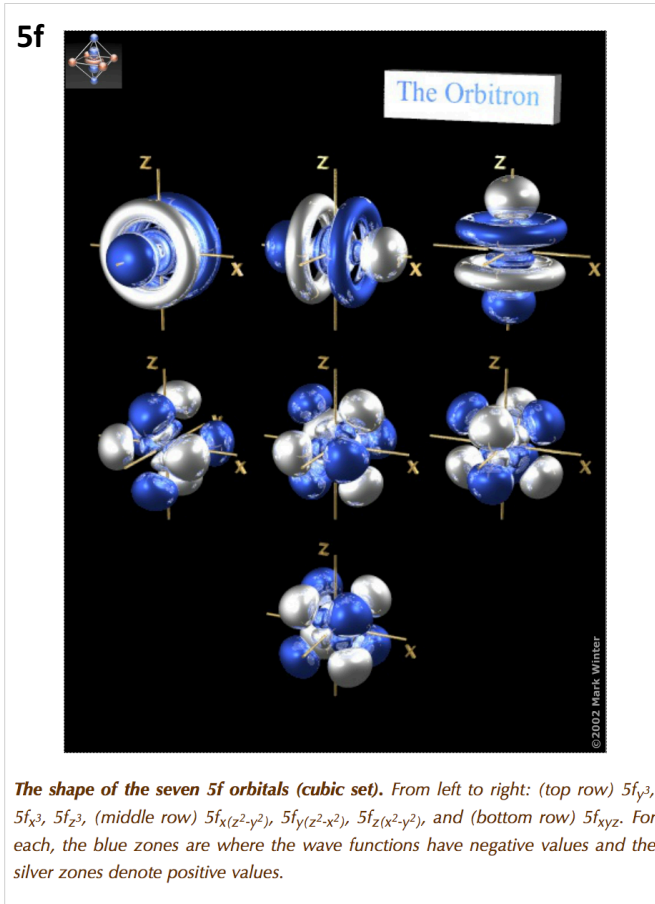
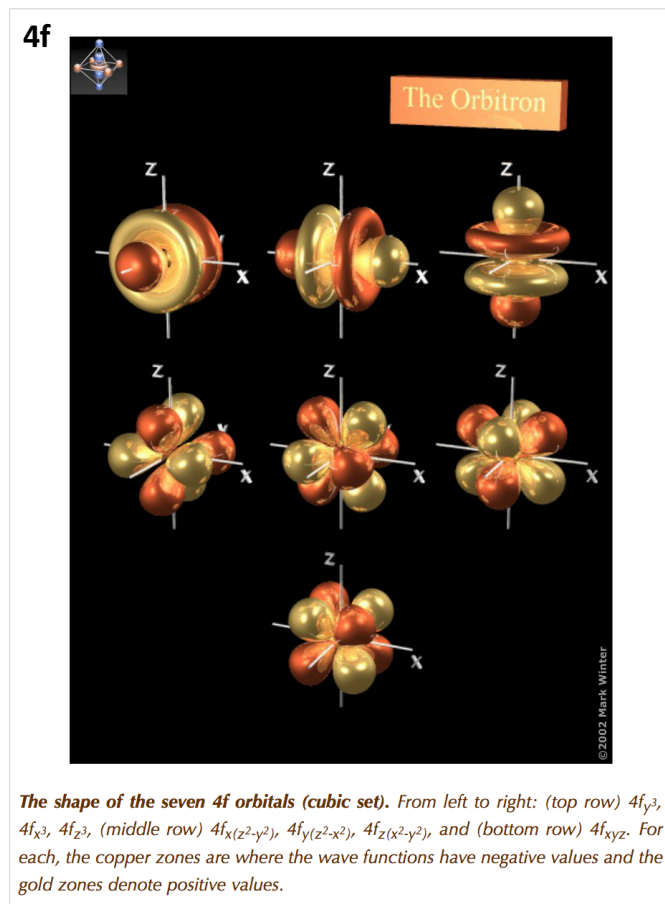
Decay Type	Radiation Emitted	Generic Equation	Model
Alpha decay	${}^4_2\alpha$	${}^A_ZX \longrightarrow {}^{A-4}_{Z-2}X' + {}^4_2\alpha$	 Parent → Daughter + Alpha Particle
Beta decay	${}^0_{-1}\beta$	${}^A_ZX \longrightarrow {}^A_{Z+1}X' + {}^0_{-1}\beta$	 Parent → Daughter + Beta Particle
Positron emission	${}^0_{+1}\beta$	${}^A_ZX \longrightarrow {}^A_{Z-1}X' + {}^0_{+1}\beta$	 Parent → Daughter + Positron
Electron capture	X rays	${}^A_ZX + {}^0_{-1}e \longrightarrow {}^A_{Z-1}X' + \text{X ray}$	 Parent + Electron → Daughter + X ray
Gamma emission	${}^0_0\gamma$	${}^A_ZX^* \xrightarrow{\text{Relaxation}} {}^A_ZX' + {}^0_0\gamma$	 Parent (excited nuclear state) → Daughter + Gamma ray
Spontaneous fission	Neutrons	${}^{A+B+C}_{Z+Y}X \longrightarrow {}^A_ZX' + {}^B_YX' + C{}_0^1n$	 Parent (unstable) → Daughters + ENERGY + Neutrons

There are 3 main decay chains that are observed in Nature: **Th, Ra and Ac series**. Each ends in a different but stable isotope of Pb. A 4th decay chain exists, that of **Np**. Due to the short half-life of ${}^{237}\text{Np}$ (2.14 M y), the chain is extinct in Nature. The ending isotope is ${}^{205}\text{Tl}$. The decay chains are schematically shown below.



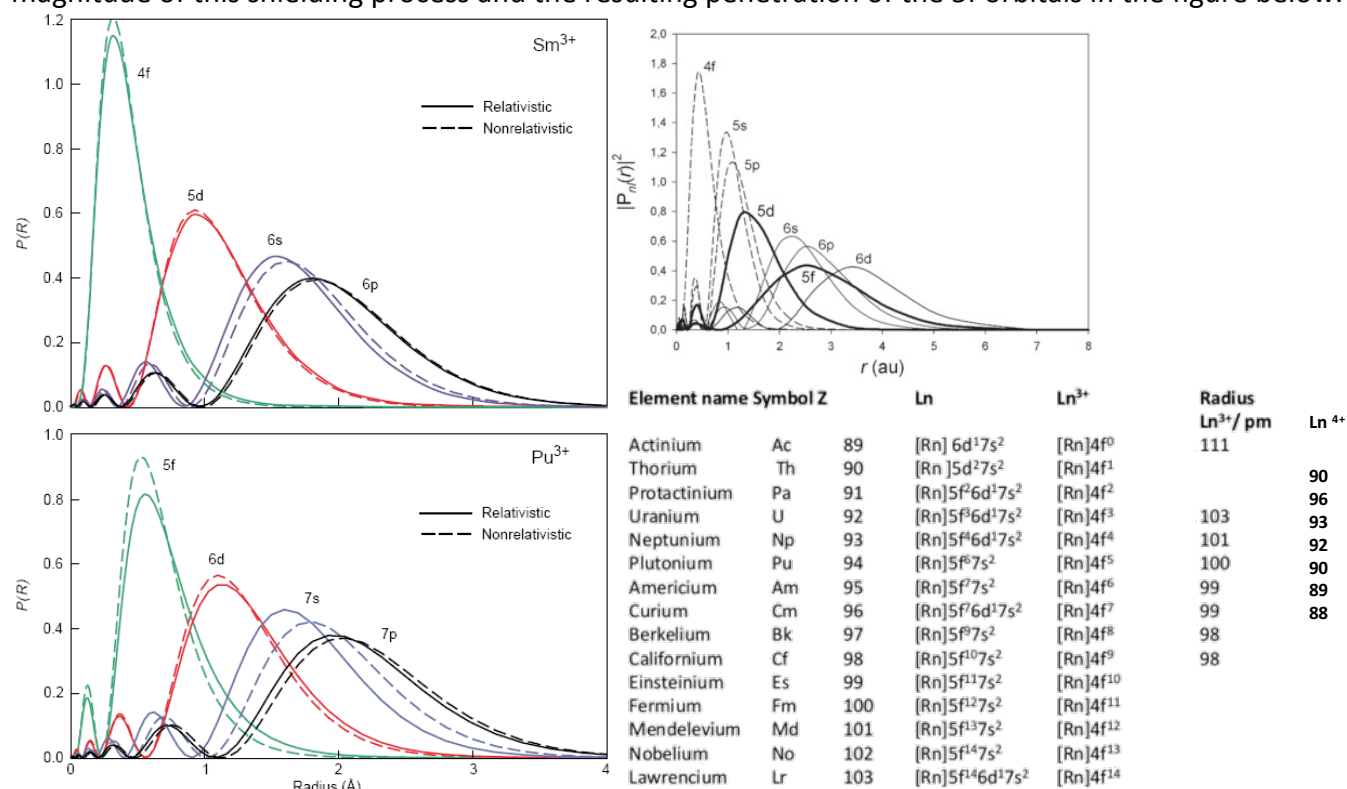
6.2 Electronic configuration of actinoids

The 5-f-orbitals are very similar in shape and symmetry to the 4f orbitals of the lanthanoids. These are shown below.



There exists likewise an actinoid contraction, with the 5f orbitals acting very much like core electrons due to the poor shielding of the 5f orbitals. The 7s, 7p and 6d orbitals are themselves all positionally overlap while 5f, 6d, 7s, 7p all of comparable energies. Therefore, it is often impossible to say which orbital is involved in bonding (observe the electronic configuration of each of the An elements

below). As with lanthanoids, actinoids are also influenced by relativistic effects. We can observe the magnitude of this shielding process and the resulting penetration of the 5f orbitals in the figure below.



6.2 Properties of actinoids (An)

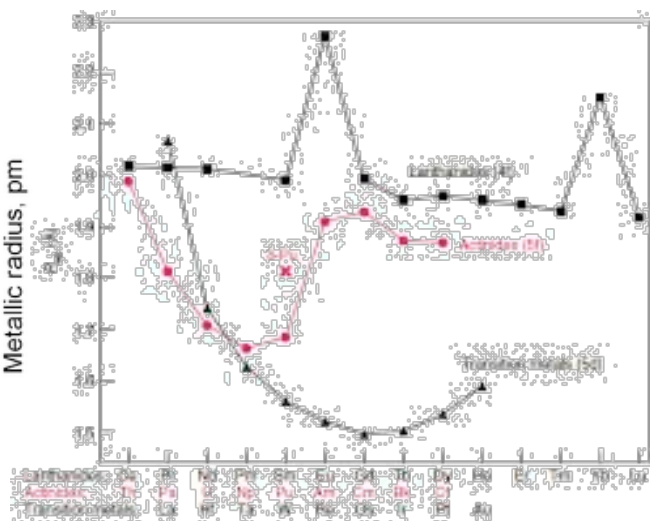
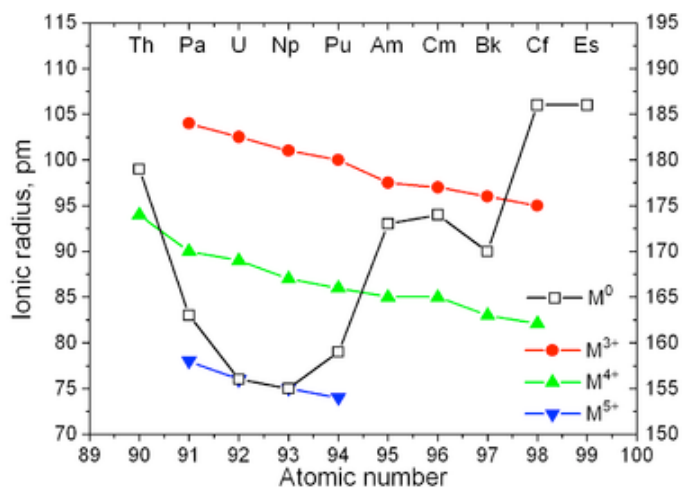
The major oxidation state (OS) for An is 3+. Some show OS of 4+ (Th). U, Np, Pu and Am can be 6+ An²⁺ are rare and show similar properties to Ln²⁺ and Ba²⁺. Pa is mainly +5. Np and Pu can be 7+.

For early actinoids, promotion 5f → 6d occurs to provide more bonding electrons. This is much easier than the corresponding 4f → 5d promotion in lanthanoids. Covalent bonding and bonding w/ π-ligands possible (e.g., UF₃ covalent but not NdF₃). The second half of the actinoid series resembles lanthanoids more closely.

The magnetic properties are more complex than with lanthanoids but actinoids are **paramagnetic**. Actinoids have high Mp and Bp but there are no trends observed. Th through Np are very similar to transition metals in their chemistry.

The geometries around actinoid metals are similar to Lanthanoids e.g., both Ce and Th have distorted icosahedral (C.N. = 12) geometry while C.N. = 8, 9 are very common [UF₈]²⁻, Th(S₂CNEt₂)₄. Generally, a wide range of C.N. and oxidation states is available to actinoids.

The ionization potentials for actinoids are also very similar to those of lanthanoids.



6.3 Some facts about actinoids

Thorium:

- It is widely dispersed (> 3 ppm of the Earth's crust)
- Natural Th is essentially 100% ²³²Th
- Occurs mainly in monazite and in uranothorite (as a mixture of Th and U silicates)

Uranium:

- It is widely distributed (mostly in igneous rock)
- Natural U is 99.27% ²³⁸U and .72% ²³⁵U
- It is usually found as UO₂
- It is mainly used for nuclear fuel and for colouring glass/ceramics

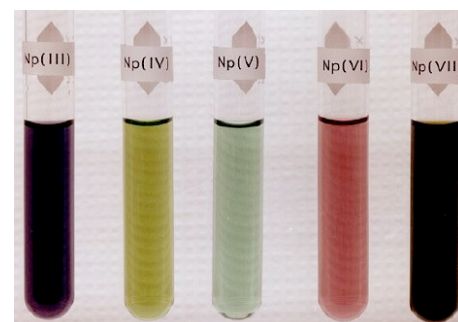
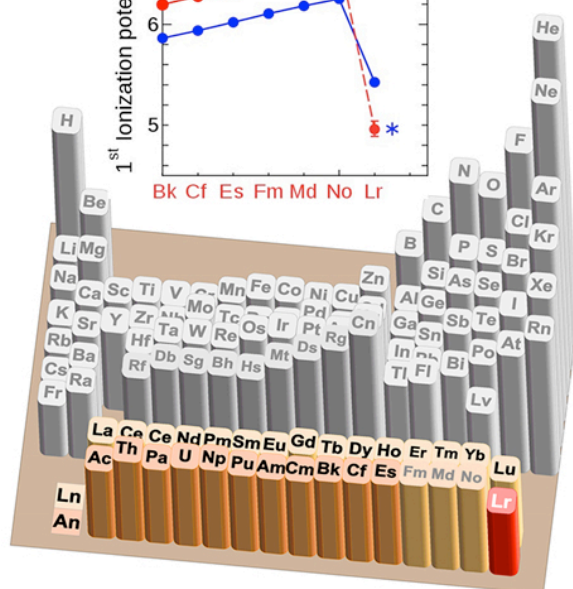
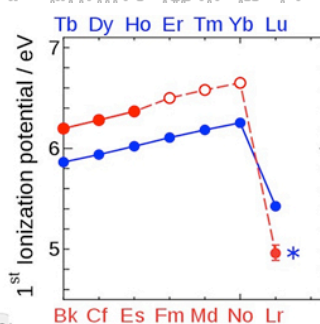
Plutonium:

- ²³⁹Pu is produced from ²³⁸U by neutron capture in nuclear reactors
- It can be further processed for nuclear weapons
- It is used as a compact energy source due to heat generated from α-decay (e.g., deep sea diving suits)
- It was used during the Apollo space mission and in human heart pacemakers
- When combined with PbTe, it is a completely reliable for producing electricity

Americium:

- ²⁴¹Am is used as the α-emission source in smoke alarms

6.3 Absorption properties of actinoids



As with lanthanoids, the absorption spectra of actinoids show a series of narrow bands that is, relatively speaking, not influenced by ligand field effects. The ϵ are 10x those of Ln bands. The spectra are complex to interpret.

7 A brief overview of metals in medicine

H																	He	
Li	Be											B	C	N	O	F	Ne	
Na	Mg											Al	Si	P	S	Cl	Ar	
K	Ca	Sc	Ti	V	Cr	Mn	Fe	Co	Ni	Cu	Zn	Ga	Ge	As	Se	Br	Kr	
Rb	Sr	Y	Zr	Nb	Mo	Tc	Ru	Rh	Pd	Ag	Cd	In	Sn	Sb	Te	I	Xe	
Cs	Ba	La	Hf	Ta	W	Re	Os	Ir	Pt	Au	Hg	Tl	Pb	Bi	Po	At	Rn	
Fr	Ra	Ac	Rf	Db	Sg	Bh	Hs	Mt										
			Ce	Pr	Nd	Pm	Sm	Eu	Gd	Tb	Dy	Ho	Er	Tm	Yb	Lu		
			Th	Pa	U	Np	Pu	Am	Cm	Bk	Cf	Es	Fm	Md	No	Lr		

essential elements for man (symbols in white font); medical radioisotopes (green fill); elements currently used in therapy (blue fill); diagnosis (orange fill). from *Chem. Commun.*, **2013**, *49*, 5106-5131.

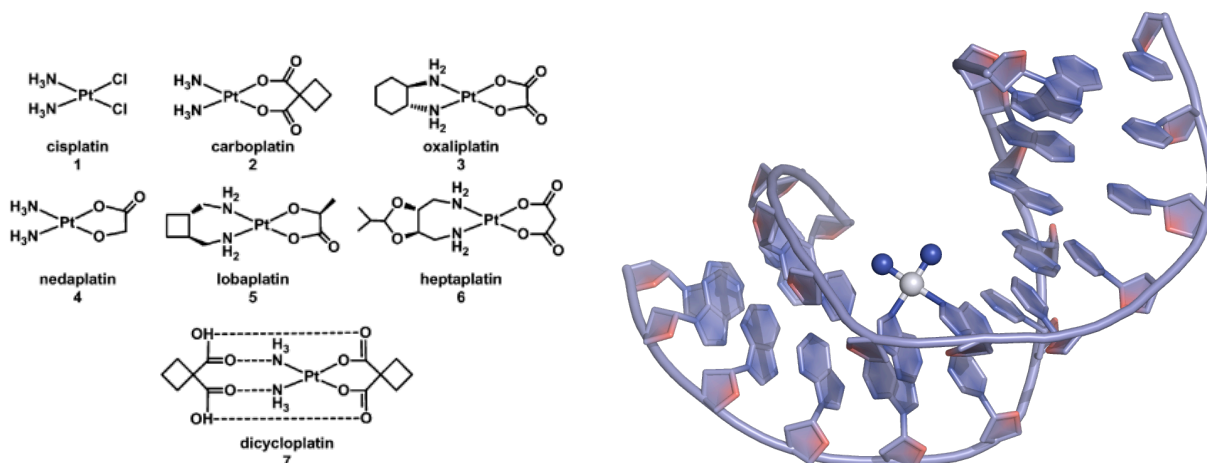
As can be observed above, transition metals and lanthanoids find myriad uses in medicine, be they as components of drugs, in luminescent or radioimaging for diagnostics or even in radiotherapeutics.

The following sections highlight some classical examples. However, this is by no means an exhaustive account of metals used in medicine.

7.1 Pt based drugs

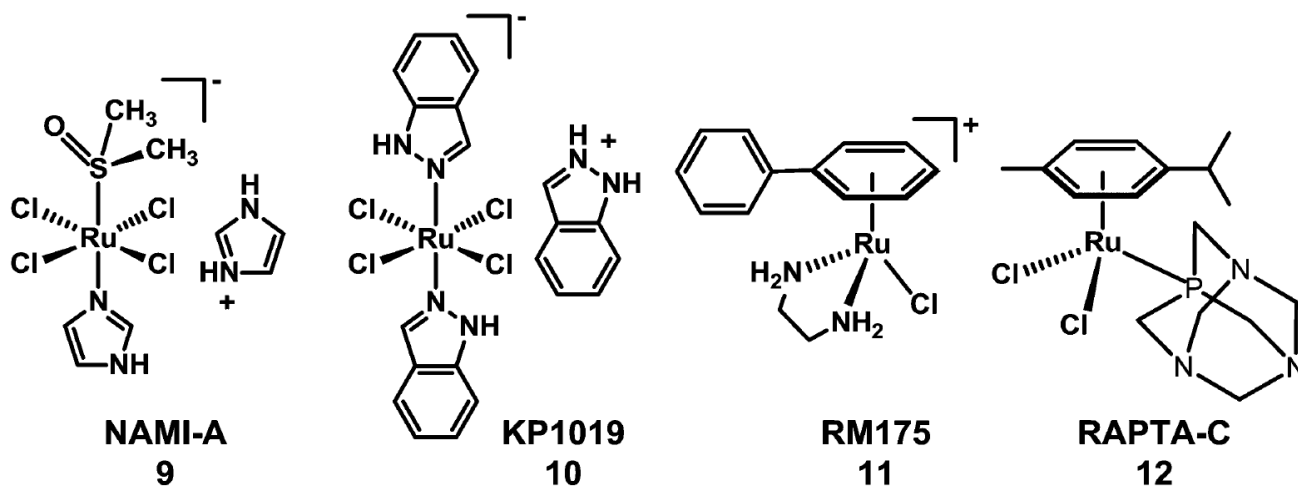
Since 1978, cisplatin is one of the most used anti-cancer drugs. It is primarily targeted in treatment of testicular and ovarian tumors. Broadly speaking, it works by forming both inter- and intra-strand crosslinks via guanidine alkylation. Mechanistically, the chloride ligands hydrolyse under biological conditions in an associative mechanism to give an aqua complex. Cisplatin promotes bending (kinking) of duplex up to 45° by unwinding of the helix at platination site, widening and flattening of the minor groove opposite the platinum adduct.

Carboplatin was invented in 1986 and shows less severe side nausea and vomiting. Oxaplatin shows activity against some cisplatin-resistant cancers and came to market in 1996.



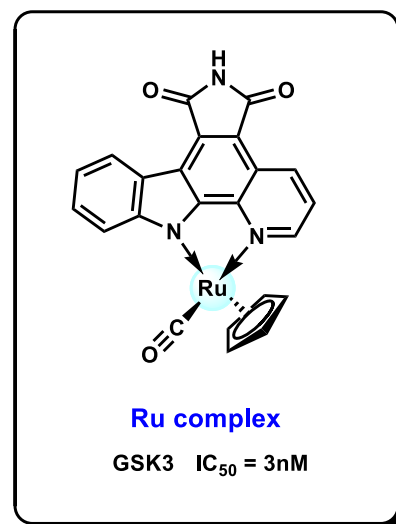
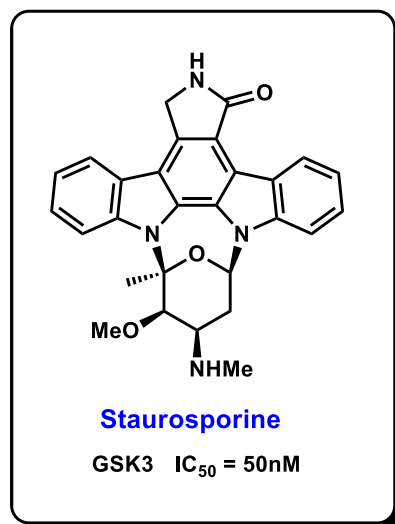
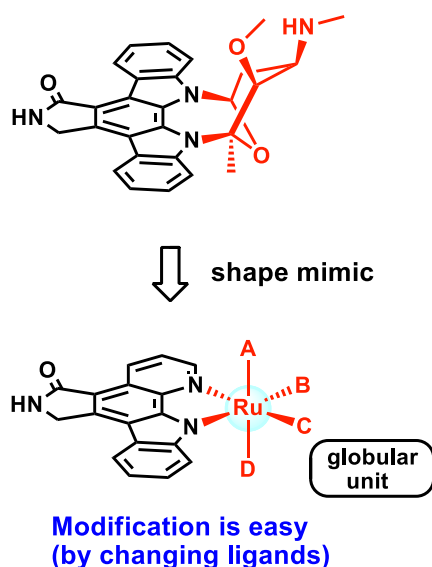
7.2 Ru based drugs

As ruthenium is in the same group as iron, ruthenium complexes are able to take advantage of the body's ability to efficiently transport and uptake of iron. In recent years, ruthenium-based molecules have emerged as promising antitumor and antimetastatic agents. Ruthenium compounds are usually less toxic and no cross-resistant than platinum counterparts, therefore better tolerated *in vivo*. In animal models, ruthenium compounds are effective in the treatment of cancer types, which cannot be treated by platinum compounds, most probably due to a different mode of action.



The above Ru drugs control of angiogenesis (possibly because it interferes with NO metabolism) and anti-invasive properties towards tumor cells. DNA binding can involve not only direct coordination to G bases but also arene intercalation in the case of RM175.

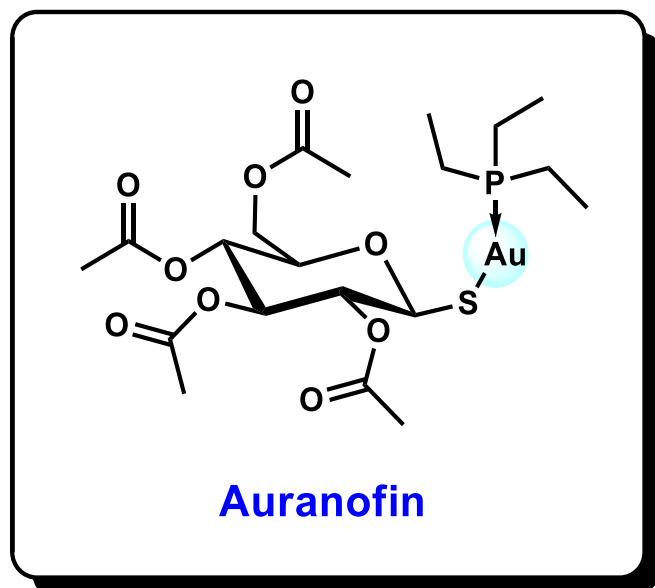
Staurosporine is known as a nonspecific protein kinase inhibitor. By replacing the globular carbohydrate unit of staurosporine with Ru fragment, a series of selective inhibitors of GSK3 were discovered.



Chem. Commun., 2013, 49, 5106--5131

7.3 Au based drugs

Auranofin is an oral drug approved for treating rheumatoid arthritis in 1985. Gold drugs show anti-inflammatory effects and inhibition of tissue degradation. The affinity of Au(I) for thiolate, and hence protein binding to methionine or cysteine, may be responsible for some effects on the immune system.



Auranofin strongly inhibits *Plasmodium falciparum* growth, which is the protozoan agent of human amebiasis, probably due to a direct inhibition of *Plasmodium falciparum* thioredoxin reductase.

Presently, there are trials planned towards the treatment of amoebiasis and parasite *Giardia intestinalis*. Amebiasis is the fourth leading cause of death due to protozoan infections worldwide, resulting in 70,000 deaths annually.

7.4 Diagnostic radiopharmaceuticals - Technetium

Radioisotopes are used in medical imaging and therapeutics, pending on the energy of the radiated energy (see below). By far the most important and common source of radiopharmaceuticals is technetium (Tc). Technetium is the only human-made element in the d-block and is radioactive.

It is formed by bombarding ⁹⁸Mo with neutrons and γ -rays in a nuclear reactor. This forms ⁹⁹Mo, which then undergoes β^- decay in 2.8 days to form metastable ^{99m}Tc (m for metastable). This metastable

Radiation Type	Energy	Wavelength	Use in Medicine
Alpha – α (He^{2+})	2-10 MeV	μm	Therapy
Beta – β	1-3 MeV	mm	Therapy
Beta ⁺ – β^+ (γ)	(511 keV γ)	(γ m)	Imaging (PET)
Gamma – γ	0.05 - 2 MeV	M	Imaging (SPEC)
X-ray – X	0.1 - 130 keV	dm	Imaging (CAT)

species, with a $t_{1/2}$ of 6 hours then undergoes γ -emission to form ^{99}Tc . The energy of this γ -emission is on the order of 140 keV, which is ideal for imaging. ^{99}Tc itself decays via β^- decay to ^{99}Ru with a very long half-life of 2.1×10^5 years.

Below is a sample of the Tc complexes used for diagnostics, particularly for heart imaging.

Therapeutic radiopharmaceuticals are useful for delivering locally cytotoxic doses of ionising radiation.

The radionuclides used emit β^- particles (electrons) or α -particles (used in targeted α -therapy (TAT)).

Most radiotherapeutic nuclides in the clinic are β^- emitters, such as ^{32}P , ^{47}Sc , ^{64}Cu , ^{67}Cu , ^{89}Sr , ^{90}Y , ^{105}Rh , ^{111}Ag , ^{117}Sn , ^{131}I , ^{149}Pm , ^{153}Sm , ^{166}Ho , ^{177}Lu , ^{186}Re , ^{188}Re .

